

**An Interactive Site Modeling Tool for Estimating
Coverage Regions for Wireless Communication Systems
in Multifloored Indoor Environments**

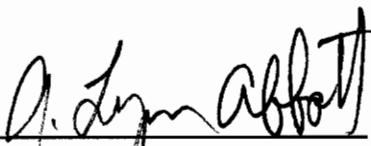
by

Manish A. Panjwani


**Thesis submitted to the faculty of the
Virginia Polytechnic Institute and State University
in partial fulfilment of the requirements for the degree of**

**Master of Science
in
Electrical Engineering**


Approved:



A. Lynn Abbott, Chairman



Theodore S. Rappaport



Brian D. Woerner

May 22, 1995

LD
5655
V855
1995
P365
C.2

An Interactive Site Modeling Tool for Estimating Coverage Regions for Wireless Communication Systems in Multifloored Indoor Environments

by

Manish A. Panjwani

A. Lynn Abbott, Chairman

Electrical Engineering

Abstract

For indoor wireless communication systems, RF transceivers need to be placed strategically to achieve optimum communication coverage at the lowest cost. Unfortunately, the coverage region for a transceiver depends heavily on the type of building and on the placement of walls within the building. Traditionally, therefore, transceiver locations have been selected by human experts who rely on experience and heuristics to obtain the optimum (or near-optimum) placement.

This thesis describes an interactive software system that can be used to assist in transceiver placement. It is intended to be easy to use by individuals who are not experts at wireless communication system design. After the user has selected transceiver locations within a graphical floor plan, the system interprets the floor plan and uses simple path loss models to estimate coverage regions for each transceiver. These regions are highlighted, enabling the user to assess the total coverage. This thesis describes the methodology used to compute the coverage regions for multifloored buildings. The effect of interference sources on coverage regions has also been analyzed using simple propagation prediction models. The resulting system is expected to be useful in the deployment of indoor wireless systems.

Acknowledgments

My sincere appreciation goes to my academic advisor, Dr. A. Lynn Abbott. His guidance and support during the past two years have provided me with an invaluable experience. For dialogue, feedback, and encouragement, I wish to thank Dr. T. S. Rappaport. I also extend my appreciation to Dr. B. D. Woerner for serving on my graduate committee.

This work would not have been possible without the preceding contributions of Dr. S. Y. Seidel and I thank him for his doctoral work that provided the foundation for this research. This research was supported in part by AT&T Global Information Solutions (formerly NCR), Utrecht, the Netherlands. For this, I also wish to thank Mr. J. Haagh of AT&T GIS.

I wish to acknowledge the support of Brian Frank, Vikram Shrivastava, Ken Farrar, Keshav Ratwani, Carl Dietrich, Nisha Sharma, and Nitin Bhat during different stages of this work. I also wish to thank my friends Rajesh Bhojwani and Divya Prakash for providing the support and encouragement which I very much needed at times during the course of this research.

I dedicate this work to my late grandfather, Dr. A. Ratwani, who has influenced me more than he could have ever realized. Finally, I give my greatest appreciation to my parents, Anand and Sadhana Panjwani, and my brother Vishal, for their love, support, and encouragement which allowed me to get this far in my academic career.

Table of Contents

Abstract	ii
Acknowledgments.....	iii
Table of Contents	iv
List of Figures.....	vi
List of Tables	ix
1. Introduction.....	1
1.1 Indoor Wireless Communication Systems	2
1.2 The Indoor Radio Propagation Channel.....	5
1.3 Design Issues in Indoor Wireless Communication Systems	6
1.4 Motivation	6
1.5 Contributions of this Research.....	8
2. An Overview of the Site Modeling Tool.....	11
2.1 Project Goals.....	11
2.2 Problem Formulation.....	12
2.3 Modules of the Site Modeling Tool	12
2.4 AutoCAD as a Graphical Foundation.....	15
2.4.1 Introduction.....	15
2.4.2 AutoCAD Terminology	16
2.4.3 AutoCAD Development System.....	17
3. Modules of the Site Modeling Tool	19
3.1 Environment Description Module	19
3.1.1 Introduction.....	19
3.1.2 Transceiver Communication Parameters.....	21
3.1.3 Receive Filter Characteristics for Interference Sources	21
3.2 RF Channel Module	23
3.2.1 Large-Scale Path Loss Models	23
3.2.2 Overview of Path Loss Models used	25
3.2.3 Single-Floor Models	27
3.2.4 Multifloor Models.....	28

3.2.5 Other Models.....	31
3.3 Communication Module.....	32
3.3.1 Overview.....	32
3.3.2 Communication Feasibility Model.....	33
3.4 Site Coverage Module.....	35
3.5 User Interface Module.....	36
4. Site Modeling Tool Operational Features.....	40
4.1 Operation of the Site Modeling Tool.....	40
4.2. Site Modeling Tool Commands.....	42
4.2.1 Placement Commands.....	42
4.2.2 Environment Attribute Commands.....	45
4.2.3 Multifloor Control Commands.....	47
4.2.4 Program Control Commands.....	48
4.2.5 Additional Commands.....	50
5. Site Modeling Tool Operational Examples.....	52
5.1 Examples of Operation.....	52
5.2 Accuracy Assessment.....	57
5.3 The Effect of Contour Resolution.....	61
5.4 Operating Speed of the Site Modeling Tool.....	65
5.4.1 Examples of Operating Speed.....	65
5.4.2 Estimating Coverage Region Calculation Times.....	70
6. The Effect of Interference Sources.....	71
6.1 Introduction.....	71
6.2 The Simplified C/N and C/I Contours.....	71
6.3 The Effect of Interferers on Coverage Regions.....	75
6.4 An Improved Search for Coverage Contours?.....	83
6.5 Variation in Coverage Areas.....	84
7. Conclusion.....	88
References.....	92
Appendix A: List of SMT Program Files.....	95
Appendix B: SMT Code Compilation.....	97
Vita.....	99

List of Figures

Fig. 1.1-1: Transceivers (base stations) and portable users within a building [Cox85].....	3
Fig. 1.5-1: Example floor plan showing the coverage region of a transceiver (□) that has been placed interactively in a hallway of an AutoCAD floor plan. The two dark contours represent different thresholds of the received signal level. The building layout greatly affects the shape of the coverage region.....	9
Fig. 2.2-1: The actual estimated transceiver coverage region S and the approximating boundary polygon P	13
Fig. 2.3-1: Modules of the Site Modeling Tool. The User Interface provides interactive control of all other modules. The Building Description module contains information that is used by the RF Channel, Communication, and Site Coverage modules.....	14
Fig. 3.1.3-1: Receive filter gain curve for interference sources at 915 MHz.....	22
Fig. 3.2.1-1: A typical received waveform in buildings showing small-scale fading and average signal strength over a local area [Sei92a].....	24
Fig. 3.2.4-1: Empirically determined values of floor attenuation factors (FAF) [Sei92a-c] as a function of the number of floors of separation between the transmit and receive points.....	30
Fig. 3.4-1: Pseudocode of the algorithm used to determine communication feasibility at a point.....	37
Fig. 4.2-1: The SMT screen menu. These abbreviations have been chosen because AutoCAD limits menu items to 8 characters.....	43
Fig. 5.1-1: Example floor plan. This is one floor of Whittemore Hall on the Virginia Tech campus. This drawing was generated directly from an AutoCAD file provided by the university's Facilities Planning and Construction department.....	54
Fig. 5.1-2: Coverage contours for one transceiver. Unnecessary details have been removed from the drawing in the previous figure, and concrete partitions only are assumed. Notice that the coverage area is reduced near regions where many partitions are present. The drawing is more appealing when viewed in color on the PC's monitor.....	54
Fig. 5.1-3: Coverage contours for repositioned transceiver. The transceiver of the previous figure has been moved to the right by a small amount.....	55
Fig. 5.1-4: Effect of single-tone interferer. The transceiver has not moved from its location in Fig. 5.1-3. The coverage area is changed considerably by the interference source.....	55
Fig. 5.1-5: Addition of coverage contours for transceiver on different floor. Transceivers not on the floor being viewed are distinguished by squares with thinner lines. The coverage area is nominally circular, but is perturbed here by the interference source.....	56

Fig. 5.1-6: Second example floor plan. This is one floor of Virginia Tech's Veterinary Medicine building. Three transceivers have been placed as a first attempt to provide complete floor coverage.....	56
Fig. 5.2-1: Measurements at 1.3 GHz. The 9 locations labeled A through I represent receiver locations on the second floor of Whittemore Hall (Adapted from [Sei92a]).....	58
Fig. 5.2-2: Measurements at 4.0 GHz. The 21 locations labeled A through U represent receiver locations on the second floor of Whittemore Hall (Adapted from [Sei92a]).....	58
Fig. 5.3-1: Coverage region for a transceiver obtained by determining only 9 boundary points.	63
Fig. 5.3-2: Coverage region for the same transceiver obtained by determining 18 boundary points. This angular resolution provides a reasonably good first order estimate of the coverage region.	63
Fig. 5.3-3: Coverage region obtained by determining 36 boundary points. This angular resolution is most often sufficient to provide a very good working estimate of the coverage region.	64
Fig. 5.3-4: Coverage region obtained by determining 72 boundary points. This angular resolution may be used for higher resolution in highly cluttered areas if 36 boundary points do not suffice.....	64
Fig. 5.3-5: Coverage region obtained by determining 180 boundary points. This angular resolution, although very impressive, might actually be a little inaccurate.	65
Fig. 5.4.1-1: Relative plots of the time taken to calculate a coverage region as a function of the number of boundary points for different values of d_{res} . The transceiver was placed at the location shown in Fig. 5.1-3.	69
Fig. 5.4.1-2: Relative plots of the time taken to calculate a coverage region for a transceiver only, as well as a transceiver and an interferer, as a function of the number of boundary points for $d_{res} = 2.0$ m. The transceiver and the interferer were placed at the locations shown in Fig. 5.1-4.	69
Fig. 6.2-1: (a) Signal level and (b) contour plots of U in dB. The transceiver is located at the origin.	72
Fig. 6.2-2: (a) Signal level and (b) contour plots of V in dB. The transceiver is located at the origin and the interferer is located at (40,0). The positive and negative peaks in V arise at the location of the transceiver and interferer respectively.....	73
Fig. 6.3-1: Plots of U and V as a function of x . Several threshold values of $U = u_{t1}, \dots, u_{t5}$ and $V = v_t$ are indicated, as described in Section 6.3.....	77
Fig. 6.3-2: The dark shaded areas are the coverage regions resulting from the selected values of u_t and v_t in Fig. 6.3-1. Note that S_u is <i>inside</i> the circle $U = u_t$, whereas S_v is <i>outside</i> the circle $V = v_t$	78

Fig. 6.3-3: Plots of U and V as a function of x . New threshold values of $U = u_{t6}, \dots, u_{t10}$ and $V = v_t$ are shown.	79
Fig. 6.3-4: The dark shaded areas are the coverage regions resulting from the selected values of u_t and v_t in Fig. 6.3-3. Here, S_u is <i>inside</i> the circle $U = u_t$, and S_v is also <i>inside</i> the circle $V = v_t$	80
Fig. 6.3-5: Plots of U and V as a function of x . New threshold values of $U = u_{t11}, \dots, u_{t13}$ and $V = v_t$ are shown.	81
Fig. 6.3-6: The dark shaded areas are the coverage regions resulting from the selected values of u_t and v_t in Fig. 6.3-5. In this case also, S_u is <i>inside</i> the circle $U = u_t$, whereas S_v is the entire region to the left of $V = v_t$	82
Fig. 6.5-1: Plot of coverage area ($S_u \cap S_v$) as a function of U for different v_t thresholds.	85
Fig. 6.5-2: Plot of transceiver coverage area as a function of U for (a) $v_t = 0$ dB, (b) $v_t = V_T = -6$ dB, and (c) $v_t = -12$ dB.	86

List of Tables

Table 3.1.2-1: Default transceiver communication parameter values used by the SMT..	21
Table 3.2.2-1: Summary of the variables used to predict path loss.	25
Table 3.2.3-1: Mean path loss exponent $n(\text{same floor})$ at 915 MHz for use in the (same floor) distance-dependent path loss model [Sei92b].....	28
Table 3.2.4-1: Mean path loss exponent $n(\text{multifloor})$ at 915 MHz for use in the (multifloor) distance-dependent path loss model (Adapted from [Sei92b]).....	29
Table 3.2.4-2: Mean floor attenuation factor (FAF) at 915 MHz for use in the (multifloor) floor attenuation factor path loss model (Adapted from [Sei92b]).....	31
Table 5.2-1: Measured and predicted path loss at 1.3 GHz on the second floor of Whittemore Hall (Adapted from [Sei92a]).	59
Table 5.2-2: Measured and predicted path loss at 4.0 GHz on the second floor of Whittemore Hall (Adapted from [Sei92a]).	60
Table 5.4.1-1: Coverage region calculation times as a function of distance and angular resolutions, for a single transceiver using the partition attenuation factor path loss model. The observed times will vary with the complexity of the floor plan, as well as the values of the communication parameters.	66
Table 5.4.1-2: Coverage region calculation times as a function of distance and angular resolutions, for a single transceiver using the same floor distance-dependent path loss model. The computation times are independent of floor plan complexity.	67
Table 5.4.1-3: Coverage region calculation times as a function of distance and angular resolutions, for a single transceiver and interferer using the partition attenuation factor path loss model.	67
Table 5.4.1-4: Coverage region calculation times as a function of distance and angular resolutions, for a single transceiver and interferer using the same floor distance-dependent path loss model.	67
Table 6.2-1: Values for communication parameters used in Figs. 6.2-1 to 6.5-2.	74

Chapter 1.

Introduction

This thesis describes an interactive software tool that has been developed to estimate coverage regions of transceivers or base stations for wireless communication system design in indoor environments. The system, known as the Site Modeling Tool (SMT) [Pan94], displays floor plans and permits the user to place RF transceivers at arbitrary locations within a building. The user can interactively set communication parameters and can view the resulting coverage regions which are highlighted on the floor plan using color graphics. With this visual information, the user can adjust transceiver locations and parameters for improved coverage of an entire building. The coverage regions are estimated using simple user-selectable site-specific propagation models that incorporate the effect of the locations and material properties of walls and floors. The system displays one floor at a time, but supports both single-floor and multifloor buildings.

The SMT runs in a Windows™ environment on an IBM-compatible PC. It has been developed as an extension to AutoCAD™, which is a popular graphical drawing system currently used by many architects. All SMT software has been written as C-language functions that are accessed through AutoCAD's graphical user interface.

This chapter provides a brief introduction to indoor wireless communication systems and the issues involved their design. The relevance of the SMT in this context is then outlined. Chapter 2 presents an overview of the SMT and introduces the five modules that comprise the system. A brief introductory tutorial to AutoCAD and the

reasons for using it as a foundation for the SMT are presented. Chapter 3 then describes each of the five SMT modules in detail.

Chapter 4 describes the operational features and user-selectable parameters that have been incorporated into the program. It also provides details concerning the commands available to the user. Chapter 5 presents examples that have been generated using the SMT with actual floor plans. The effect of contour resolution on the coverage regions is discussed in some detail. A brief assessment of the accuracy of the SMT is also included. Chapter 6 contains further analysis of the effect of interference sources on RF coverage regions. Finally, Chapter 7 summarizes this thesis report. Suggestions for future work that could be undertaken to improve the utility of the SMT are also outlined.

This thesis contains two appendices. Appendix A provides a list of the files that are associated with the SMT. Appendix B briefly outlines the process of compiling the SMT code.

1.1 Indoor Wireless Communication Systems

Mobile and portable communications has experienced a tremendous growth rate since about 1980. The success of cellular radio indicates that ubiquitous personal communication is indeed well on its way to becoming a reality. The estimated potential market for the deployment of wireless personal communication systems runs into billions of dollars.

A major goal of communication systems research and deployment is the creation of integrated networks. It is envisaged that such networks will share resources to convey all types of information among man and machines, irrespective of their locations. At the present time, the technology exists to transfer high information volumes within an integrated network economically. However, the bottleneck of such networks is still the

connection between the network and the user terminals. These connections have traditionally been costly and rather restrictive. Subscriber loops and building wiring are expensive to install and reconfigure. Furthermore, wired connections limit the user's mobility [Cox85, Mol91]. As a consequence, indoor wireless communication systems such as cellular mobile radio telephones and residential cordless telephones have become very popular.

As part of a complete Personal Communications System (PCS), wireless coverage will be required within buildings. The development of portable radio communication systems for indoor environments has seen a tremendous spurt of activity over the last decade. The development of such indoor systems has immediate potential for improving the point-to-point communication between and among workers and machines in office and manufacturing environments. Fig. 1.1-1 [Cox85] shows how transceivers (base stations) could be distributed in a building to help achieve this goal. The RF transceivers would be connected to a conventional wired backbone, and portable terminals or users

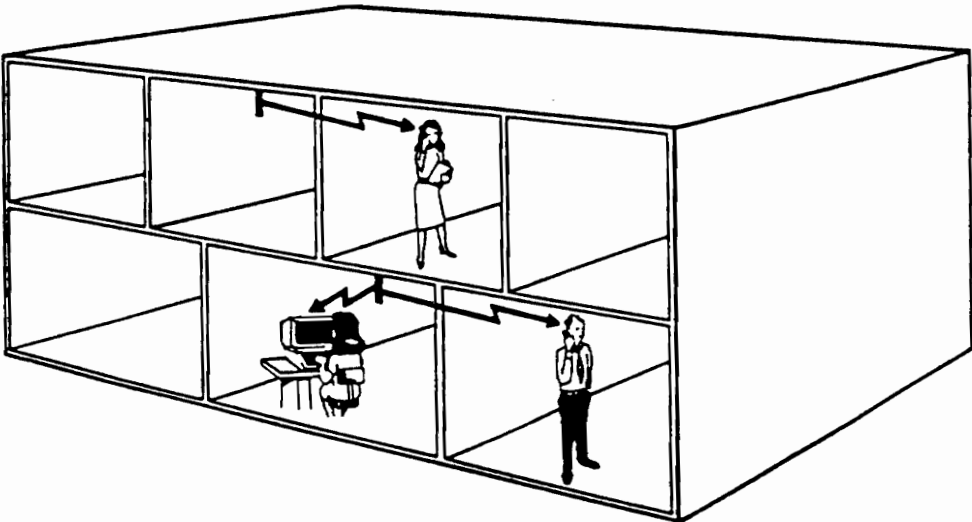


Fig. 1.1-1: Transceivers (base stations) and portable users within a building [Cox85].

would be free to be relocated or roam and continue to receive service by the strongest transceiver or base station. With such systems, people will no longer be restricted and inconvenienced by a stationary telephone in an office or a residence. The importance of these systems to the long term objective of developing worldwide personal communications is already resulting in telephones which will no longer be associated with a specific location but with individual persons. The development of modern cellular telephone systems is merely the first step in merging the best features of cordless phones and cellular radio to provide two way calling, data, voice, and video transmission services.

In addition to voice transmission, radio communication has other potential applications in indoor environments as well. As an integrated part of factories and office buildings of the future, radio communication will help in improving the efficiency of manufacturing techniques by providing reliable and efficient stationary and portable information transmission systems for a wide variety of applications. At the present time, coaxial and fiber optic cables form the backbone of the transmission medium in almost all computer and machine data links. However, the amount of cables used increases proportionally with an increase in the number of machines and hard-wired telephone systems. As a solution, the concept of wireless local area networks (WLAN's) has gained popularity in the last few years. WLAN systems incorporate one or more transceivers that are connected to a conventional cabled network backbone. These transceivers act as central controllers and communicate at RF frequencies with data terminal equipment (such as personal computers or workstations) that are placed at various locations within a building [Pan94]. Network installation, maintenance, and reconfiguration will be considerably faster with radio communication links for data transmission.

1.2 The Indoor Radio Propagation Channel

With indoor radio communications, there is rarely a line-of-sight (LOS) between the transmitter and the receiver. As a result, radio waves are attenuated and redirected as they are scattered by walls, partitions, and other physical obstacles. Furthermore, the radio propagation channel in indoor environments is continuously changing and is therefore difficult to predict.

Problems include multipath and shadowing, which reduce the coverage area as well as the quality of the received signal. In multipath propagation, the transmitted signal arrives at the receiver via several paths because of scattering, reflection, refraction, and diffraction from the physical obstacles in the surrounding environment. Such objects may be static objects like walls, partitions, and doors or even time-varying entities such as people or machinery moving around. In narrow-band communication systems, multipath propagation gives rise to Rayleigh fading which results in a signal strength variation when the receiver is spatially moved. In addition to the Rayleigh fading, there is also shadow fading that is caused by blockage and attenuation of signals by walls, doors, etc. However, this effect varies slowly with location, with fades occurring in different portions of a building. In wide-band transmissions, path delays also affect the quality of the received signal by causing frequency selective fading. In a digital communication system, the time dispersion due to delay spread results in inter-symbol interference (ISI). This ISI increases with the signaling rate and thus limits the maximum data rate for acceptable error performance. Furthermore, in buildings with multiple users, interference among users who are using the same channel in a different area can be a serious problem. This is called co-channel interference (CCI), and systems must be designed to reduce this interference to an acceptable level. Buildings thus present a rather hostile environment for radio communication.

1.3 Design Issues in Indoor Wireless Communication Systems

The characterization of the indoor radio propagation channel is the first step of the design process, and thus forms the basis for the development of reliable and efficient communication systems. Implementation of wireless indoor systems in the low microwave bands (800 MHz - 5 GHz) has sparked a large interest in understanding the propagation of radio signals within and around buildings [Hon93]. Many researchers have made measurements of radio waves and statistically modeled their results in several types of buildings for both single and multiple floors, with most of them being around 900 MHz [Cox84, Dev90, Haw90, Hon93, Laf90, Mot88, Pah89, Rap89a, Rap89b, Sal87, Sei92b, Sei92c]. The congestion of radio spectrum at this band has resulted in some work in the 1-2 GHz and 60 GHz bands for indoor systems recently [Has93]. Literature surveys of radio propagation into and within buildings are given in [And95, Has93, Mol91, Rap94].

Once the propagation is understood more thoroughly, engineers may design systems more efficiently in terms of size layout, frequency planning, and system performance. Accurate models and design tools based on these models can allow system designers to determine the appropriate modulation techniques, equalization, and multiple access techniques that are most suited for indoor wireless systems. To do this effectively, all the above mentioned characteristics of the indoor radio environment must be considered.

1.4 Motivation

In order to design an indoor wireless system, propagation characteristics must be predicted. In current systems, large numbers of measurements throughout a potential coverage region are performed, and crude statistical models are used to determine signal

characteristics. Systems must often be overdesigned which reduces efficiency in terms of frequency re-use, leading to increased system installation costs and decreased system capacity [Sei92a].

More recently, researchers have developed software tools based on statistical models to assist in the design and performance evaluation of indoor radio systems. A very good example of such a tool is SIRCIM (Simulation of Indoor Radio Channel Impulse Response Models). SIRCIM was developed by Virginia Tech's Mobile and Portable Radio Research Group (MPRG) based on work described in [Rap91]. This tool generates realistic small-scale indoor channel impulse response samples and can be used to investigate system issues such as channel access, hand-off, co-channel interference, outage probability, equalization, diversity and modulation performance, etc., in open plan building environments [Sei92a].

Tools like SIRCIM are valuable for evaluating system performance on a statistical basis at a microscopic level, but these have, until now, used only limited information about the building environment the radio system operates in. Another problem in designing a wireless system is that it can be difficult to determine how many transceivers are needed and where they should be placed within a building. For economic reasons and for radio spectrum conservation, transceivers should be strategically located so that only the desired areas of the building are covered, and so that neighboring coverage areas do not overlap significantly. Optimum placement of transceivers or base antennas is complicated by the fact that indoor propagation losses are highly dependent on the type of building and on the locations and composition of walls within the building.

This aspect of indoor radio system design calls for a design tool that must be easy to use, provide interactive graphical feedback, be fast, and use accurate site-specific

propagation path loss models to estimate the size and shape of transceiver coverage regions.

1.5 Contributions of this Research

Path loss models describe the channel at a macroscopic level and thus complement the models used by tools such as SIRCIM. To date, however, no such design tool has been described in the literature. The SMT has been primarily developed in response to this need of indoor radio system design, and is the major contribution of this research.

Ray tracing methods, such as those described in [Sei92d, Val93], can be used to predict narrow-band power delay profiles, which may then be averaged over several wavelengths to obtain the local wide-band loss between the transmitter and receiver. However, instead of relying on traditional ray tracing methods which, although more accurate, are very slow, the approach employed by the SMT utilizes simple distance-dependent and partition-dependent path loss models [Sei92b] that are sufficiently fast and accurate. Furthermore, the SMT implements these features in an interactive software package. However, for reasons explained later in Chapter 3, multipath and shadowing effects are not considered in these models.

As mentioned before, the Site Modeling Tool has been developed as an extension of AutoCAD and runs on a 486-based personal computer. The user can add, reposition, and delete transceivers, and can adjust communication parameters such as transmitting powers, carrier-to-noise thresholds, and operating frequency interactively. In order to develop a communications arrangement for a particular building, a knowledgeable applications engineer is needed. This person considers the type and size of the building, and specifies the number and placement of Access Points. A major goal of this project

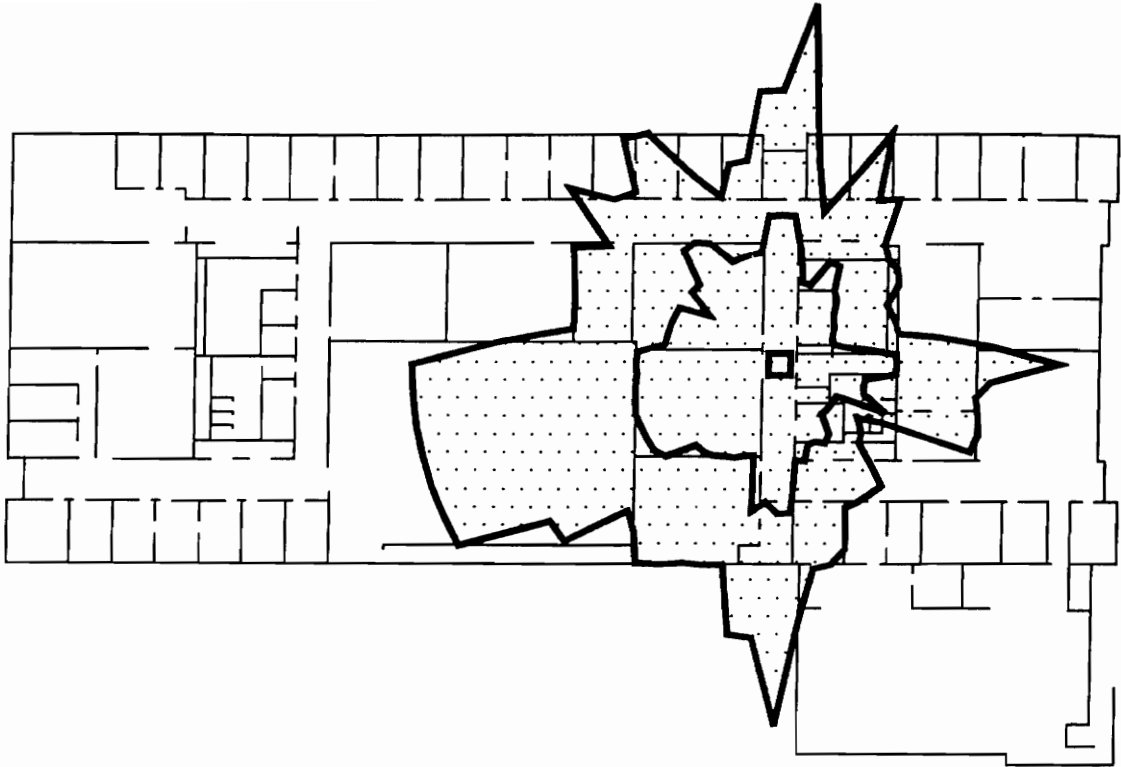


Fig. 1.5-1: Example floor plan showing the coverage region of a transceiver (□) that has been placed interactively in a hallway of an AutoCAD floor plan. The two dark contours represent different thresholds of the received signal level. The building layout greatly affects the shape of the coverage region.

was to develop a user-friendly software package that could be used by anyone to specify such a system. Fig. 1.5-1 shows an example floor plan and the estimated coverage region for a single transceiver that has been computed by the SMT. Details of the design, development, and operation of the SMT constitute the major portion of this thesis.

The FCC has reserved a number of frequency bands for unlicensed Industrial, Scientific, and Medical (ISM) devices. These bands are 902-928 MHz, 2400-2483.5 MHz, and 5725-5850 MHz. A number of products are currently available that operate in these bands under FCC's Part 15 regulations. AT&T Global Information Solutions (formerly NCR) markets a product known as WaveLAN™ in which data terminal equipment (DTE) communicate with transceivers at 915 MHz or 2.4 GHz. Each transceiver is part of an Access Point, which may be connected with other Access Points

using an Ethernet™ or Token-Ring backbone to serve as the base station for the DTE clients. The FCC is also currently in the process of awarding licenses in the PCS spectrum at 1840-1990 MHz. Thus, although the SMT can, in its present form, be used only for the 902-928 MHz and 2400-2483.5 MHz ISM bands, it is a simple matter to modify it for other frequencies as well.

Because wireless systems tend to be interference limited rather than noise limited, their capacity and performance is ultimately limited by the interference from co-channel transmitters [Car94, Rap94]. Another contribution of this research has been an analysis of the effect of interferers on the coverage area of nearby transceivers by using simple distance-dependent path loss models. This analysis provides useful insights into the extent of an interferer's effect.

To summarize: This thesis describes a software tool that serves an important need in wireless system design. It uses simple propagation prediction models to provide fast operation. It is interactive, relatively easy to use, and it operates with the popular AutoCAD system on an inexpensive PC platform. Although it is limited to two-dimensional graphics, the SMT computes coverage regions for multifloor buildings. This thesis also presents a new careful evaluation of the effect of interference sources on coverage regions.

Chapter 2.

An Overview of the Site Modeling Tool

The goals of this research are first outlined. A high-level mathematical problem statement is then formulated, followed by a brief introduction to the various modules of the SMT. Finally, an introductory tutorial to AutoCAD is presented to allow the uninitiated reader to understand the concepts relevant to the SMT in the chapters that follow.

2.1 Project Goals

The SMT was developed with a view to accomplish the following major goals:

- 1) The resulting system should calculate and display transceiver coverage areas within buildings.
- 2) The system must be interactive, easy to use, and fast.
- 3) The user must be able to place transceivers and interference sources within a displayed floor plan.
- 4) In the interest of execution speed, the system should implement simple propagation models, but should incorporate the effects of concrete walls, cloth partitions, and multiple floors.
- 5) The system should implement an appropriate communication feasibility model.
- 6) The system should be modular, to simplify later upgrades.
- 7) The system should run on a 486 PC in a Windows environment.

The SMT does not perform automatic, optimal placement of transceivers for complete RF coverage of a floor or building. This could be a long-term goal, however, as addressed in Chapter 7.

2.2 Problem Formulation

This section presents a concise mathematical formulation of the problem that the SMT must solve in order to determine the coverage region of a single transceiver. We begin by defining the predicate

$$f(x,y) = \begin{cases} 0, & \text{if communication is not feasible at } (x,y) \\ 1, & \text{if communication is feasible at } (x,y) \end{cases} \quad (2.1)$$

where (x,y) is a receiving point on a two-dimensional floor plan. The problem is to determine the region S , such that

$$S = \{(x,y) \mid f(x,y) = 1\}.$$

Let $h(x,y) = 0$ represent the boundary δS of the region S . It is assumed that that this boundary is a simple closed curve. Then, for computational purposes, the problem reduces to determining an n -point polygon P , where

$$P = ((x_0, y_0), (x_1, y_1), \dots, (x_{n-1}, y_{n-1}))$$

approximates the boundary of S . The points (x_i, y_i) represents vertices of P listed in counterclockwise order. That is,

$$P = \{(x_i, y_i) \mid h(x_i, y_i) = 0 \text{ for } i = 0, 1, \dots, n-1\}.$$

For simplicity, the SMT computes the polygon points so that they lie on (or near) the theoretical boundary predicted by the path loss models (Section 3.2), and according to the communication feasibility model discussed in Section 3.3. This is shown in Fig. 2.2-1. A different polygon must be computed for each transceiver.

2.3 Modules of the Site Modeling Tool

The SMT has been developed as five separate modules, as shown in Fig. 2.3-1.

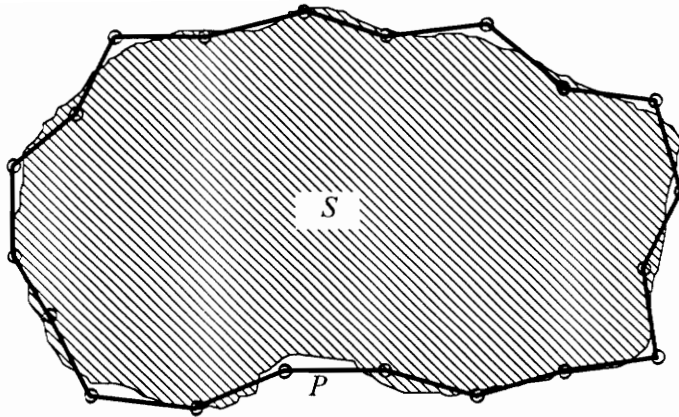


Fig. 2.2-1: The actual estimated transceiver coverage region S and the approximating boundary polygon P .

Modularity has been important for simplifying development and for testing SMT software. This approach will permit one system module to be updated at a later time without the need to redesign the rest of the system. For example, if a more sophisticated RF model (used to determine signal attenuation) becomes available in the future, this portion of the system is the only one which needs to be updated.

The Environment Description module contains all available information about the building, including the number of floors, placement of walls, and building materials used. It also maintains information about transceiver locations, interference source locations, and related communication parameters.

The RF Channel module predicts path loss in the indoor environment. When computing path loss for a given point in a building, different equations apply depending on whether the transceiver of interest is on the same floor or is on a different floor. When on the same floor, two separate (user-selectable) path loss models have been implemented. One of these is a function of the number of intervening partitions, and the

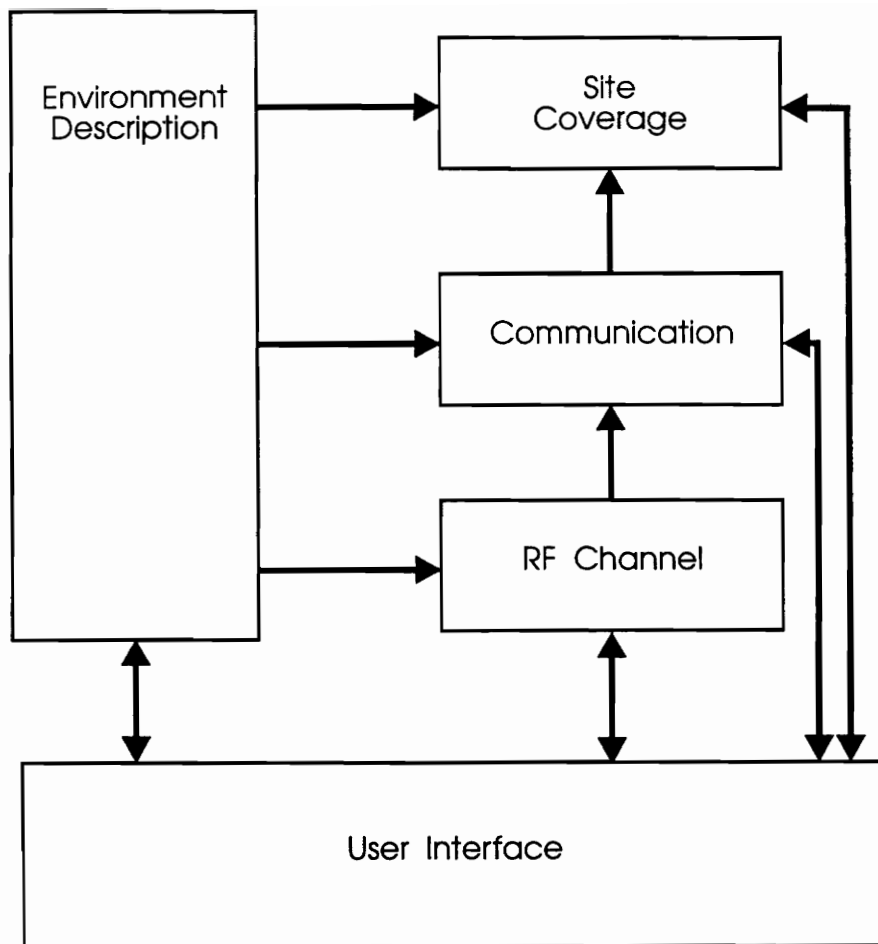


Fig. 2.3-1: Modules of the Site Modeling Tool. The User Interface provides interactive control of all other modules. The Building Description module contains information that is used by the RF Channel, Communication, and Site Coverage modules.

other depends only on distance from the transceiver. When the transceiver is on a different floor from the point of interest, two additional path loss models are used (and are also user-selectable). All of these models depend on the type of building; the currently supported environments include manufacturing plants, hospitals, and office buildings. The SMT can be used for *any* indoor environment for which sufficiently accurate propagation data is available or can be reasonably estimated from experience.

The Communication module is built as a hierarchical layer above the RF Channel module. It combines path loss predictions with additional information to predict the ability to communicate at a given point in the building. This module also takes into account the effect of small numbers of single-tone interference sources. The Site Coverage module has the task of computing the coverage regions of selected transceivers. This involves the iterative calculation of point-to-point communication feasibility, as determined by the Communication module, for many different locations in the building. The output from this module is a contour plot of the coverage region(s). The last module is the User Interface module. This module is concerned with all entry and display functions of the Site Modeling Tool. It interacts with the user, with AutoCAD, and with the other modules to coordinate all computations.

2.4 AutoCAD as a Graphical Foundation

2.4.1 Introduction

AutoCAD is a popular package for computer aided design and drafting. It is available for a wide variety of workstations and personal computers. The designers of AutoCAD have made it possible for the user to customize and extend many of the basic features of the package. It is possible to define new pull-down menus and icons, for example, and it is possible to execute external computer programs while editing a

drawing within AutoCAD. The DOS and OS/2 platforms provide 255 colors to enhance complex drawings and thus make them easier to visualize.

AutoCAD (Release 12 for Windows) was adopted as the foundation for the SMT for three main reasons: 1) It allowed us to concentrate on communication and propagation models, rather than computer graphics. This shortened the development time considerably. 2) Extensions to AutoCAD can be developed in the C language. 3) AutoCAD is a common means of representing floor plans. Floor plans for several campus buildings were easily obtained in AutoCAD form.

2.4.2 AutoCAD Terminology

Many features of AutoCAD were used in the development of the SMT. While it is not possible to discuss all of these features in this report, some of the most important concepts are introduced in this section.

A *polyline* is a set of lines that are treated as a single entity. The entire set of lines can be rotated, deleted, and edited with a single command. Polylines therefore provide a convenient way to represent and manipulate arbitrarily complex polygons. This is important because coverage region boundaries are represented in the SMT as polygons.

An AutoCAD drawing can consist of several *layers*. Each layer can be used to represent a different logical portion of a drawing. In the SMT, for example, each floor of a building uses different layers to represent concrete partitions, cloth partitions, and coverage areas separately. Each layer may be *on*, *off*, or *frozen*. Every layer that is on is visible on the monitor, similar to a set of transparent overlays that are simultaneously visible. A layer that is either off or frozen does not appear on the monitor. The fundamental difference between these two states is that AutoCAD continues to process the contents of layers that are off, but does not consider entities on a frozen layer. In

order to enhance processing speed, therefore, it is desirable within the SMT to freeze layers that are not of immediate interest. In the SMT, soft partitions, concrete walls, and coverage regions are all drawn on different layers.

2.4.3 AutoCAD Development System

The SMT was developed using the AutoCAD Development System (ADS), which is marketed by Autodesk specifically to assist third parties in developing extensions to AutoCAD. ADS provides a C-language interface in the form of an object library. The library contains approximately 85 C functions that execute standard AutoCAD commands, retrieve or set the value of AutoCAD system variables, prompt the user for input, display and activate menus, and update screen images.

In order to develop an AutoCAD extension, the user writes a new function in C that invokes functions from the ADS library. This new function is compiled and linked with the ADS code. After AutoCAD is invoked, the new function can be loaded and then executed just like any standard AutoCAD command. If desired, new functions created in this manner can be placed in pull-down menus or in a menu that is permanently displayed at the side of the screen. It is important to understand that an ADS application program will not run alone; it will only function under a running session of AutoCAD.

An ADS extension is event-driven, normally waiting within a control loop for a message from AutoCAD. When a user selects the new function, a message is sent and the user's software takes control. It is the responsibility of the new software to return control back to AutoCAD.

Several sample ADS applications are included with the AutoCAD software package. Using these example programs allows a programmer to easily create the

framework of an ADS application and concentrate on the function code, and not worry about the interface control loop and message processing.

Chapter 3.

Modules of the Site Modeling Tool

As outlined in Section 2.3, the SMT has been developed as five relatively independent modules. Each of these modules is described in this chapter. The subject of path loss models is considered in some detail, since this forms the computational basis for the SMT. The communication parameters and their default values that the SMT uses are then described. The communication feasibility model developed to determine coverage boundaries is also explained.

3.1 Environment Description Module

3.1.1 Introduction

The Environment Description module essentially serves as a database containing building information and communication parameters that may be accessed by all other modules of the Site Modeling Tool as needed. Conceptually, this module may be subdivided into 1) a building description component, and 2) a communication description component. For the first of these, useful attributes include construction material (concrete walls, cloth partitions, etc.) for given parts of the building. Other attributes that are stored here include partition attenuation factors, and the distance between floors if the building comprises more than a single story.

The communication description component maintains the locations of transceivers and single-tone interference sources. In addition to communication parameters, other attributes that are stored here include the estimated signal propagation path loss, received carrier-to-noise ratio, and received carrier-to-interference ratio. The default parameter values that the SMT uses are listed below in Section 3.1.2. After the boundary points for

coverage regions have been computed for a specific transceiver location, they are stored here as well.

In order to improve accuracy and execution speed of the SMT, a convention was developed for using AutoCAD layers to represent floor plans. Each layer is referenced within the SMT by name. (AutoCAD is not case sensitive.) Unfortunately, architects do not follow any single convention. The user may therefore need to modify an AutoCAD floor plan before using it with the SMT.

Specifically, the convention is as follows: The layer that is named "Floor f " must contain concrete walls that are located on floor f , where $f = 1, 2, 3, \dots$. The numbering must be sequential, with $f = 1$ representing the ground floor. Similarly, the layer named "Spart f " must contain soft (cloth covered) partitions that are located on floor f . All of the Floor f and Spart f layers must be provided by the user. At least one of these layers is needed for each floor, but it is not necessary to have both layers for each floor.

The SMT creates several new layers as needed. One layer is called "Icons," on which the SMT stores graphical icons for all transceivers and interference sources that are entered by the user. These are represented by small squares (■) and diamonds (◆), respectively. When the user directs the SMT to compute coverage region(s), both an outer coverage contour and an inner coverage contour are generated. These are stored on two layers named "Ocntr f " and "Icntr f ," respectively. These are discussed more thoroughly in Section 4.1. Briefly, the outer contour represents the thresholds of $C/N = 18$ dB or $C/I = 10$ dB, whichever is lower, as determined by the RF Channel module. The inner contour normally represents a received signal threshold of 10 dB *above* the outer contour, but this difference may also be adjusted by the user.

The user is free to add any number of additional layers to the drawing, so long as different names are used. These could be used to represent doors, furniture, outside

walkways, text, or anything else of interest. When using the SMT these additional layers should be frozen so that they will be ignored by the SMT. If these layers are not frozen, then accuracy will not be affected, but computation speed and aesthetic appearance will suffer.

3.1.2 Transceiver Communication Parameters

As described in Section 1.5, the SMT currently supports transceivers operating in the 900 MHz and 2400 MHz ISM bands. The default communication parameters of these transceivers are shown below in Table 3.1.2-1. Each of these values can also be adjusted interactively by the user to suit his or her needs.

Table 3.1.2-1: Default transceiver communication parameter values used by the SMT.

<i>Variable</i>	<i>Description</i>	<i>Value at 915 MHz</i>	<i>Value at 2440 MHz</i>	<i>Units</i>
n	Mean path loss exponent	2.0	2.0	-
P_t	Transmit power	24	20	dBm
BW	Receiver bandwidth	13	13	MHz
C_{\min}	Receiver sensitivity	-72	-75	dBm
$(C/N)_{\min}$	Minimum carrier-to-noise ratio	18	10	dB
$(C/I)_{\min}$	Minimum carrier-to-interference ratio	18	10	dB

3.1.3 Receive Filter Characteristics for Interference Sources

The receive filter gain curve for interference sources used by the SMT in the 915 MHz band is shown in Fig. 3.1.3-1. The gain is 6 dB at the center frequency of 915 MHz, and drops off linearly at the rate of 1 dB for every 1 MHz of deviation from the center frequency. If an interference source operates at a frequency that is outside the

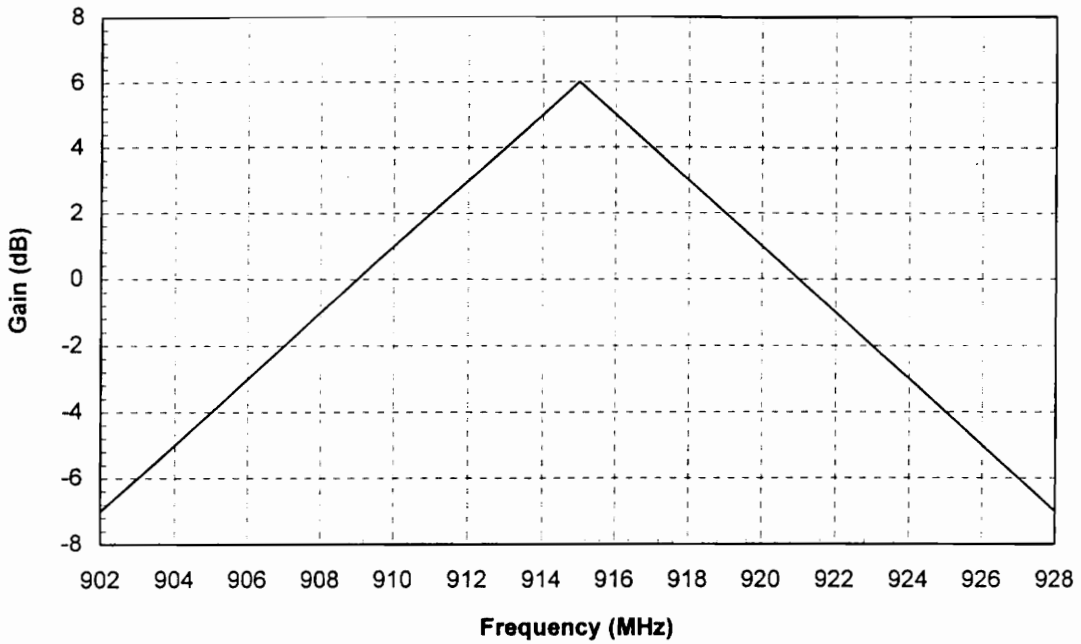


Fig. 3.1.3-1: Receive filter gain curve for interference sources at 915 MHz.

bandwidth of the 915 MHz transceiver (i.e. <902 MHz or >928 MHz), it is completely ignored and thus has no effect on the coverage regions. This can be mathematically stated as

$$G = \begin{cases} f - 909, & 902 \leq f \leq 915 \text{ MHz} \\ 921 - f, & 915 < f \leq 928 \text{ MHz} \\ \text{undefined}, & \text{elsewhere} \end{cases}$$

where G is the gain in dB, and f is the interferer frequency in MHz.

At 2440 MHz, the SMT uses a gain curve for interference sources that is identical in shape to the one shown in Fig. 3.1.3-1. However, despite the 13 MHz bandwidth of the 2440 MHz transceiver (Table 3.1.2-1) which is used only in the computation of the

noise power N , the SMT does not limit this curve to any specific bandwidth. Thus, mathematically

$$G = \begin{cases} f - 2434, & f \leq 2440 \text{ MHz} \\ 2446 - f, & f > 2440 \text{ MHz} \end{cases}$$

Thus, for an interference source operating at 2420 MHz, the transceiver would have a gain of

$$6 \text{ dB} - (20 \text{ MHz}) \times (1 \text{ dB/MHz}) = -12 \text{ dB}.$$

Similarly, although the effect of some interference sources will be insignificant, the SMT will nonetheless assign to the transceiver a very small gain for this interferer.

While the SMT currently allows the user to choose only between one of the above two hard-coded receive filter characteristic gain curves, it is a simple matter to edit the corresponding function and mathematically define any other gain curve that the user may wish to use for future upgrades of the SMT.

3.2 RF Channel Module

3.2.1 Large-Scale Path Loss Models

At this point, it is important to understand the precise implication of the quantities predicted by the path loss models employed by the SMT. We have seen that propagation within buildings has a rather complex multipath structure. This is primarily because of the building structure, layout of the room, the type of construction materials used, and even the age of the buildings. Because of the varying multipath at a receiving location on account of all these factors, the movement of a receiver unit over small spatial distances in indoor environments results in a rapid fluctuation of the received signal level. This phenomenon is termed as small-scale fading. However, to estimate coverage regions, we are interested in the average or mean signal strength. This is obtained by averaging the

received small-scale signal over receiver movements of typically 5-40 wavelengths [Cox84]. These averaging distances are chosen so that the small-scale fading will not influence the mean path loss [Sei92a].

As the receiver moves away from the transmitter, this local average signal will gradually decrease in strength, and it is this signal that is predicted by the models considered in the following sections. Since these models average signal strength over distances larger than the signal wavelength at large transmitter-receiver separations, they are referred to as *large-scale* models. Fig. 3.2.1-1 shows a received signal that fades rapidly [Sei92a]. The local mean signal, averaged over 20λ , is also shown. This represents the signal level that the large scale models used attempt to approximate. From this discussion, it is now apparent why multipath propagation is not an issue in estimating coverage regions, and has therefore not been considered in the SMT.

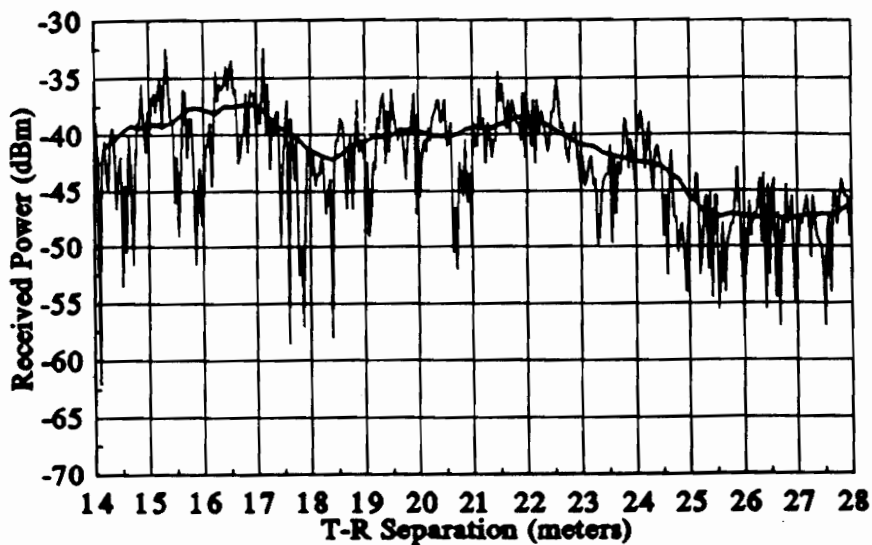


Fig. 3.2.1-1: A typical received waveform in buildings showing small-scale fading and average signal strength over a local area [Sei92a].

3.2.2 Overview of Path Loss Models used

Table 3.2.2-1 lists the parameters that are used in this section.

Table 3.2.2-1: Summary of the variables used to predict path loss.

<i>Variable</i>	<i>Description</i>	<i>Units</i>
d	Distance separating transmit and receive points	m
d_0	Reference distance	m
PL	Path loss	dB
\overline{PL}	Mean path loss	dB
n	Mean path loss exponent	—
λ	Carrier wavelength	m
p	Number of soft partitions in path	—
q	Number of concrete partitions in path	—
AF_p	Attenuation factor per soft partition	dB
AF_q	Attenuation factor per concrete partition	dB
FAF	Floor attenuation factor	dB

A common model often used by researchers to estimate path loss expresses the mean path loss \overline{PL} as a function of distance d to the power n :

$$\overline{PL}(d) \propto \left(\frac{d}{d_0}\right)^n \quad (3.1)$$

Here, n specifies the path loss behavior for a particular type of building, and d_0 is a close-in reference distance (described below). In free space, $n = 2$. When plotted on a log-log scale, this power law relationship is a straight line with a slope of $10n$ dB/decade, and the exponent n becomes multiplicative.

The mean path loss is defined as the path loss in dB from the transmitter to the reference distance d_0 plus the additional path loss described by (3.1) in decibels [Cox84, Dev90, Haw90, Lee82, Rap89a, Rap89b, Sal87, Sei92a-c].

$$\overline{PL}(d) = PL(d_0) + 10 \times n \times \log_{10}(d/d_0) \quad [\text{dB}]. \quad (3.2)$$

In microcellular and indoor environments, a reference distance of $d_0 = 1$ m is typically used [Haw90, Sei92a, Sei92b]. This reference distance should be chosen so that it lies in the far field of the transmitting antenna. For the SMT, all signal levels are referenced to this distance as follows:

$$PL(d_0) = 20 \times \log_{10} \left(\frac{4\pi d_0}{\lambda} \right) \quad [\text{dB}]. \quad (3.3)$$

The reference path loss $PL(d_0)$ is assumed to be due to free space propagation from the transmitter to d_0 . For the SMT transceivers, $PL(d_0) = 31.7$ dB at 915 MHz, or $PL(d_0) = 40.2$ dB at 2440 MHz. Measurements show that these values predicted by (3.3) are accurate to within 1 dB nominally [Rap89].

Furthermore, local large-scale path loss is often log-normally distributed about the mean power level described by (3.2) [Lee82]. That is,

$$PL(d) = \overline{PL}(d) + X_\sigma \quad [\text{dB}]. \quad (3.4)$$

X_σ is a zero-mean log-normal (normal in dB) random variable with standard deviation σ in dB. This distribution describes the random shadowing effects referred to as log-normal shadowing. Log-normal shadowing is used to account for the fact that the received signal level at different locations having the same transmitter-receiver separation will be different depending on the level of clutter along the propagation path. The standard deviation σ of X_σ does provide a quantitative measure of the accuracy of the model used to predict path loss, and is often quoted along with a model for a given set of field measurements.

It would be a simple matter to simulate log-normal shadowing by the addition of a log-normal random value with the desired standard deviation to (3.2). However, since we are interested in the *mean* path loss, this is not required in the SMT because the random variable term has a zero mean.

Several researchers have attempted to modify (3.1) in order to obtain a better empirical fit (smaller σ) to their measured data for different indoor environments and thus characterize additional site-specific information. A universally accepted indoor path loss model is not yet available. The SMT therefore incorporates the use of four effective and popular channel models proposed by Seidel and Rappaport [Sei92a, Sei92b]. These models utilize relatively simple prediction rules to estimate the large-scale signal loss between any two points inside a building based on the effects of walls, office partitions, floors, and building layout. Two of the models are valid when the transmitter and receiver are on the same floor, and the remaining two models apply when different floors are involved. In this site modeling system, the user may choose which model to use.

3.2.3 Single-Floor Models

Distance-Dependent Path Loss Model: This model does not depend explicitly on the partition locations in the floor plan, and is the same as the one described by (3.2) above. Instead, different values for the path loss exponent $n(\text{samefloor})$ are used depending on the type of building. It may be rewritten as

$$\overline{PL}(d) = PL(d_0) + 10 \times n(\text{samefloor}) \times \log_{10}(d / d_0) \quad [\text{dB}]. \quad (3.5)$$

For the SMT, the user selects the appropriate building environment, and the program assumes a value for n that has been empirically determined. Reported values for n in indoor environments vary considerably from 1 for LOS paths up to 6.5 for highly obstructed paths [Has93]. Several suggested values incorporated in the SMT are shown in Table 3.2.3-1. The user may also enter a value for n directly.

Partition Attenuation Factor Path Loss Model: This model is similar to the one proposed in [Mot90] for floors and walls. It assumes that the signal attenuates as in free space ($n =$

Table 3.2.3-1: Mean path loss exponent n (same floor) at 915 MHz for use in the (same floor) distance-dependent path loss model [Sei92b].

<i>Type of building</i>	<i>n</i>
Office building	2.8
Factory	2.2
Grocery store	1.8
Retail store	2.2
User defined site	2.0

2), and attributes all additional path loss directly to intervening cloth covered soft partitions and concrete walls:

$$\overline{PL}(d) = PL(d_0) + 10 \times n(\text{freespace}) \times \log_{10}(d / d_0) + p \times AF_p + q \times AF_q \quad [\text{dB}]. \quad (3.6)$$

Here, the term "hard partitions" (or "concrete walls") is used to refer to immovable partitions that are a part of the building structure. "Soft partitions" are those which do not generally span the ceiling and may be moved, resulting in a reconfigurable floor plan. Partition attenuation factors, typically ranging from 2 dB for aluminium slidings to 13 dB for a concrete block wall, and as large as 30 dB for corrugated steel structures have been reported in the literature [Has93]. The default SMT values for AF_p and AF_q are 1.4 dB/partition and 2.4 dB/partition respectively [Sei92b], but can also be adjusted interactively by the user.

3.2.4 Multifloor Models

Both multifloor models are used only when the transmit and receive locations are on different floors of the building.

Distance-Dependent Path Loss Model: This model is similar to (3.5), except that a larger value of n is chosen to account for the increased attenuation of intervening floors. This may be represented as follows:

$$\overline{PL}(d) = PL(d_0) + 10 \times n(\text{multifloor}) \times \log_{10}(d / d_0) \quad [\text{dB}]. \quad (3.7)$$

The values for $n(\text{multifloor})$ used in the SMT are listed below in Table 3.2.4-1. The SMT uses the same value of $n(\text{multifloor})$ for floor differences of three or more between a transceiver and a receive point.

Table 3.2.4-1: Mean path loss exponent $n(\text{multifloor})$ at 915 MHz for use in the (multifloor) distance-dependent path loss model (Adapted from [Sei92b]).

	n
Through 1 floor	4.2
Through 2 floors	5.0
Through 3 or more floors	5.3

Floor Attenuation Factor Path Loss Model: This model is also similar to the first model described in Section 3.3.2. However, the additional path loss caused by intervening floors is now added explicitly as the quantity FAF :

$$\overline{PL}(d) = PL(d_0) + 10 \times n(\text{samefloor}) \times \log_{10}(d / d_0) + FAF \quad [\text{dB}]. \quad (3.8)$$

Several values for FAF for up to five floors of separation have been reported in the literature, and some of these have been plotted in Fig. 3.2.4-1 [Sei92a-c]. Typical values for FAF , which is a function of the number of intervening floors, are about 15 dB for one floor of separation and an additional 6-10 dB for every additional floor up to five floors. There is no significant increase in FAF for more than five floors of separation, and this has been attributed to the scattering of radio energy from surrounding buildings or the diffraction of radio energy along the sides of a building [And95]. The values of FAF that the SMT uses are stored as a look-up table and are shown in Table 3.2.4-2.

Based on the current body of literature, there appear to be no significant effects of frequency on path loss for the same floor models [Sei92b]. The values of FAF , however, have been observed to be smaller at 900 MHz than at 1.7 GHz by about 6 dB [Mot88].

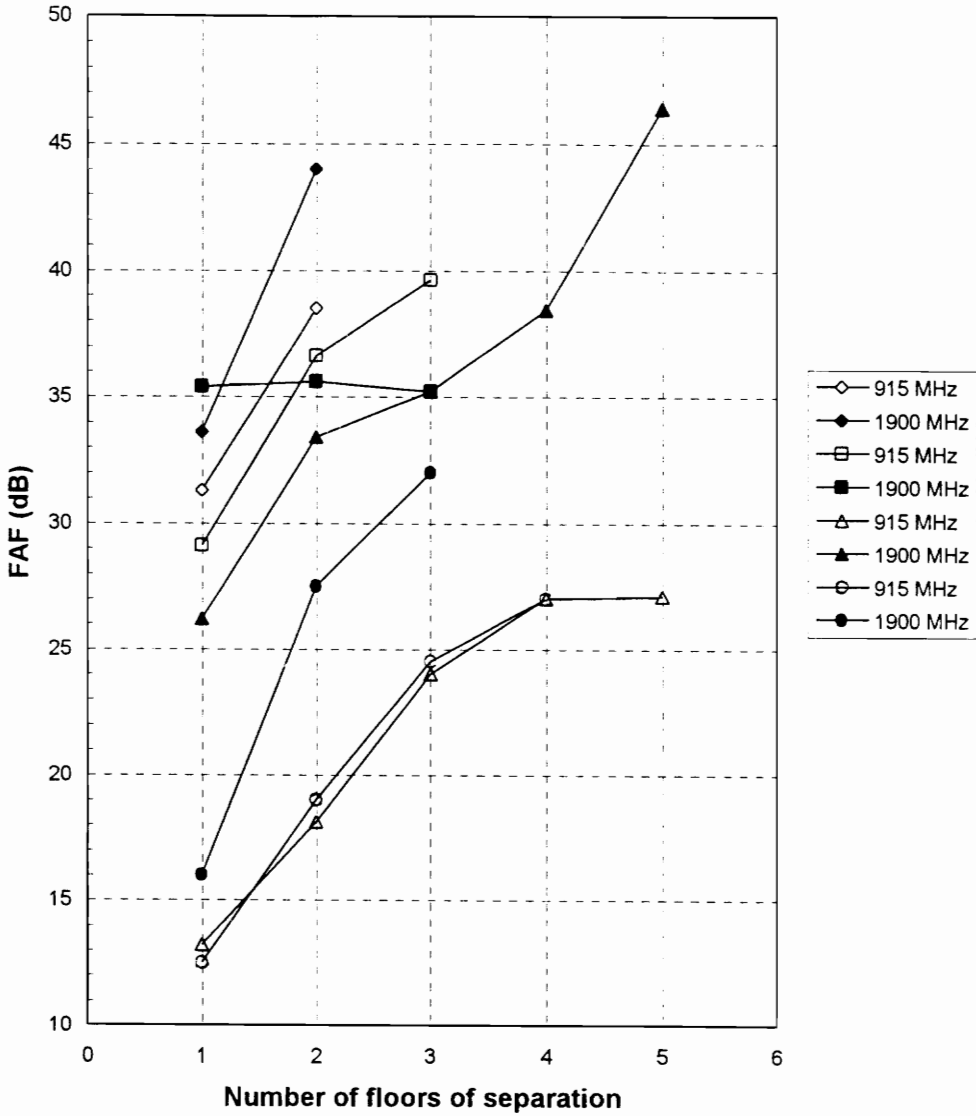


Fig. 3.2.4-1: Empirically determined values of floor attenuation factors (*FAF*) [Sei92a-c] as a function of the number of floors of separation between the transmit and receive points.

Irrespective of the operating transceiver frequency, the SMT uses the above tabulated values for computing coverage regions. Additional values for n and *FAF* in the case of multifloor environments have been listed in [And95, Sei92b, Sei92c].

Table 3.2.4-2: Mean floor attenuation factor (*FAF*) at 915 MHz for use in the (multifloor) floor attenuation factor path loss model (Adapted from [Sei92b]).

	<i>FAF</i> (dB)
Through 1 floor	13.2
Through 2 floors	18.1
Through 3 floors	24.0
Through 4 floors	27.0
Through 5 or more floors	27.1

3.2.5 Other Models

Devasirvatham, et al. have proposed another distance-dependent model that models path loss as d^2 plus α dB/m. That is [Dev90]

$$\overline{PL}(d) = PL(d_0) + 20 \times \log_{10}(d / d_0) + \alpha \times d \quad [\text{dB}].$$

Reported values for α range from 0.3-1.2 dB/m, with no clear dependence on frequency [Has93].

In yet another model proposed by Ericsson, the parameter n is not considered a constant for a given environment, but varies with distance. In this break-point model, the value of n changes at discrete points at specified distances from the transmitter.

Although simple to implement, these models have not been included in the SMT for lack of sufficient data, as well as the inability of these models to explain α in terms of site-specific parameters like the models discussed above in Sections 3.2.2 and 3.2.3.

Before concluding this section, it is important to note that the SMT considers only *in-in* building propagation. Thus, no special consideration is given to transceivers or interference sources that may have been placed outside the building perimeter on the floor plan, or to parts of coverage regions that may "spill" outside. The perimeter walls of a building are treated as just another partition.

3.3 Communication Module

3.3.1 Overview

This module predicts communication feasibility for a given point within a building. Communication feasibility at a given point is defined as the ability to receive a signal which exceeds the minimum required carrier-to-noise, receiver sensitivity, and (if any interference sources are present) carrier-to-interference thresholds by a specified margin, and which therefore allows acceptable communication quality. It relies heavily on estimates of signal attenuation from the chosen RF channel model on the given floor plan, and utilizes information provided by the Environment Description module.

In order to determine whether communication is feasible, it is necessary to compare the received carrier power C and carrier-to-noise ratio C/N with the receiver sensitivity C_{\min} and minimum required carrier-to-noise ratio $(C/N)_{\min}$ at the point under consideration. The likely allocation of only a limited range of radio frequencies for a particular wireless indoor system will require extensive frequency reuse within buildings in order to support many users. Since co-channel interference is the dominating factor in limiting capacity, it is essential to understand, estimate, and incorporate its influence on the coverage regions. Therefore, if a small number of single-tone interference sources (co-channel transmitters) are present, the received carrier-to-interference ratio (co-channel interference) C/I is compared with the minimum allowed value $(C/I)_{\min}$. Communication is deemed feasible if the received signal levels are all above the minimum user-specified thresholds. Electromagnetic equipment such as computers, CRTs, elevators, TVs, and microwave ovens are often found near transceivers and add to the ambient noise. Therefore, the calculation of noise power N , in addition to thermal noise, also incorporates the effect of this environmental noise. Recent studies indicate

that the mean power level of this noise is typically about 18 dB above the thermal noise floor [Bla93].

3.3.2 Communication Feasibility Model

The communication feasibility model is now developed algebraically. Consider a transceiver with transmit power P_t and a receiving point at a distance d_t from the transceiver. The carrier power C at the receiving point is given by

$$C = P_t - \overline{PL}(d_t) \quad [\text{dBm}], \quad (3.9)$$

and the white noise P_n present at the receiver input is given by

$$P_n = kTB \quad [\text{dBm}],$$

where $k = 1.38 \times 10^{-23}$ J/K is Boltzmann's constant, T is the absolute room temperature, and B is the RF channel bandwidth.

Also consider the effect of environmental noise P_e on the carrier-to-noise ratio. The total noise power at the receiving point is therefore

$$N = P_n + P_e \quad [\text{dBm}],$$

and the overall input carrier-to-noise ratio will be given by

$$\frac{C}{N} = \frac{C}{P_n + P_e} = \frac{C}{kTB + P_e} \quad [\text{dB}]. \quad (3.10)$$

Now consider m single-tone interference sources¹, each having transmitting with power P_i ($i = 1, 2, \dots, m$) and at a distance d_i from the receiver. The interference power I_i at the receiver due to any single interference source is given by

¹ It is possible that two or more transceivers could be operating at the same or a similar frequency, thus resulting in co-channel interference. However, the SMT does not automatically take this into consideration while calculating C/I , and the user must place additional interferers at the transceiver locations to model this co-channel interference if desired.

$$I_i = P_i - \overline{PL}(d_i) \quad [\text{dBm}]. \quad (3.11)$$

We assume that interferers may be added on a power basis. The total interference power at the receiving point due to all the interference sources is then given by

$$I = k_1 I_1 + k_2 I_2 + \dots + k_m I_m = \sum_{i=1}^m k_i I_i \quad [\text{dB}], \quad (3.12)$$

where the coefficients k_i are determined by the transceiver receive filter characteristics described in Section 3.1.3. The overall received carrier-to-interference power at the receiver input can now be written as

$$\frac{C}{I} = \frac{C}{\sum_{i=1}^m k_i I_i} \quad [\text{dB}]. \quad (3.13)$$

Let us now define variables U , V , and W as follows:

$$U = \left(\frac{C}{N} \right) - \left(\frac{C}{N} \right)_{\min} \quad [\text{dB}] \quad (3.14)$$

$$V = \left(\frac{C}{I} \right) - \left(\frac{C}{I} \right)_{\min} \quad [\text{dB}] \quad (3.15)$$

$$W = C - C_{\min} \quad [\text{dB}] \quad (3.16)$$

With these definitions, communication is deemed feasible at a point if the following condition is satisfied:

$$\{ [(U > 0) \text{ and } (V > 3)] \text{ or } [(U > 3) \text{ and } (V > 0)] \} \text{ and } \{ W > 0 \}. \quad (3.17)$$

The value of 3 dB shown is commonly used as a practical threshold in the industry [Tuc93]. If no interference sources are present, then V is not needed and (3.17) reduces to

$$(U > 0) \text{ and } (W > 0). \quad (3.18)$$

Depending on the exact $(C/N)_{\min}$, C_{\min} , and N specifications, the smaller of the threshold contours of U and W determines the area of influence of the transceiver. Conditions (3.16) and (3.17) are analogous to equation (2.1).

3.4 Site Coverage Module

This module predicts regions of coverage within a building and displays these regions directly on the floor plan. By definition, the coverage region for a transceiver is the set of nearby points for which communication is feasible, as determined by condition (3.17) in Section 3.3.2 above. By default, the SMT assumes that signals propagate equally in all directions from a transmitter. The default coverage region, in the absence of partitions and interferers, is therefore circular for a given floor (or spherical if three dimensions are considered). When interference sources are present, or when walls are present and the partition-dependent path loss model is used, the default circular shape is perturbed according to the associated attenuation factors and C/I thresholds. The SMT further assumes that coverage regions are always connected sets without holes — no "islands" are present in a coverage region, and a single coverage region is never subdivided into separate, noncontiguous regions. These are safe assumptions in most practical situations. Chapter 6 analyzes these and additional degenerate cases that arise when interference sources are in close proximity to a transceiver.

With these assumptions, it is sufficient to detect the points near the boundary of the coverage region. The boundary will be a simple closed curve; it is assumed that communication is feasible for every point enclosed by the curve. Since the exact shape of the coverage region is not known in general, a search must be performed to locate border points. For computational reasons and for graphical highlighting on the floor plan, the boundary may be closely approximated by the vertices of a polygon, as described in Section 2.2.

In order to estimate the boundary of a coverage region, the Site Coverage module searches for vertices of the approximating polygon along lines that radiate from the transceiver's location. The search lines are uniformly spaced. Normally 18 border points are found, although the number is user-selectable. However, as described in Section 5.3, it has been observed that increasing the number of border points to more than 36 does not significantly improve the coverage prediction, except perhaps in heavily partitioned environments. It is also relatively computationally prohibitive to increase the number of points substantially.

Without loss of generality, assume that the transceiver is located at the origin of a two-dimensional Cartesian coordinate system. The first boundary point is found along the x axis. To accomplish this, an initial point is first chosen at the reference distance d_0 along the x axis. Points at intervals along the x axis are evaluated until communication is no longer feasible. At this time, the first boundary point is assumed to lie at the midpoint of the two points most recently evaluated.

For subsequent points, the search occurs along an adjacent radial line, beginning at the same distance from the transceiver as the most recently detected border point. The search proceeds toward or away from the transceiver, depending on the communication feasibility of the newly evaluated point. The search process ends after all boundary points have been located along each radial search line. This is summarized in the pseudocode shown in Fig. 3.4-1.

3.5 User Interface Module

As emphasized before, one of the primary goals in developing the SMT was to make it interactive and easy to use so that it can be used by non-experts in wireless communication design. It is the User Interface module that provides a simple interactive

mechanism for controlling the operation of the SMT. It allows the user to set building and communication parameters, place transceivers and interference sources, move from floor to floor, and direct the calculation of coverage areas. This module provides textual and graphical feedback to the user via the command line and/or specially created dialog boxes, and directs the operation of all other SMT modules.

```

1.  algorithm Locate_Boundary_Points (user provides distance resolution
    (dist_res >  $d_0$ ) and number of polygon vertex points (vtxpts))
2.  angleincr := 360/vtxpts, dist := dist_res, angle := 0
3.  repeat until angle > 360
4.      pt1 := (dist_res,  $\angle$ angle)
5.      sub-algorithm Locate_Radial_Boundary_Point
6.          if communication is feasible at pt1
7.              while communication is feasible at pt2
8.                  pt1 := pt2, dist += dist_res, pt2 := (dist,  $\angle$ angle)
9.                  check communication feasibility at pt2
10.             end while
11.          end if
12.          if communication is not feasible at pt1
13.              while communication is not feasible at pt2
14.                  pt1 := pt2, dist -= dist_res, pt2 := (dist,  $\angle$ angle)
15.                  if dist <= dist_res
16.                      print "error; interferer too close to
                            transceiver;" abort
17.                  end if
18.                  check communication feasibility at pt2
19.              end while
20.          end if
21.      end Locate_Radial_Boundary_Point
22.      vertex_pt := midpoint(pt1,pt2); put vertex_pt into array
23.      angle += angleincr
24.  end repeat
25.  array contains the list of vertex points
26.  end Locate_Boundary_Points

```

Fig. 3.4-1: Pseudocode of the algorithm used to determine communication feasibility at a point.

Since the SMT has been developed as an extension to AutoCAD, the user interface relies heavily on AutoCAD to provide an operating environment. A mouse and keyboard are used as input devices, and feedback is provided on the monitor of the PC.

Some of the more prominent provisions of this module are as follows:

- Because AutoCAD serves as the foundation of the system, full AutoCAD functionality is available to the user. The user can therefore enter floor plans from scratch, or import them from files.
- The user can interactively add, reposition, and delete any number of transceivers and interference sources.
- The user can initiate the calculation of coverage regions for a selected or all transceivers that have been placed on a floor plan. These regions are highlighted graphically and in color on the floor plan. The user may then also clear selected or all coverage regions if desired.
- The user can view and change the default communication parameter values for both transceivers as well as interference sources.
- The user can select an "environment type," such as office building or warehouse, as described in Section 3.2.3.
- The user can experiment with different path loss models.
- The user can interactively set values for $n(\text{multifloor})$, partition, and floor attenuation factors.
- The user may change the displayed contour resolution to improve SMT operation in open-plan or heavily cluttered environments.

- If the floor plan supports multiple floors, the user may move between, place transceivers and interference sources on, and view the resulting coverage regions on any floor.

These capabilities are effected by the execution of several specially developed SMT commands. All these commands are described in detail in the following chapter.

Chapter 4.

Site Modeling Tool Operational Features

This chapter begins by outlining the sequence of steps required to operate the SMT. Each SMT command that was developed is then described in detail. The capabilities and limitations of each command are also pointed out.

4.1 Operation of the Site Modeling Tool

After a drawing has been prepared as described in Section 3.1, the SMT may be used as follows. First, the user must run AutoCAD. The user must then open a floor plan, and load the SMT application. The SMT is loaded by invoking the AutoCAD "Load" command. (The SMT must be reloaded every time a new AutoCAD drawing file is opened.) This may be selected from the "File" menu, the "SMT" menu, or may be typed on the command line at the bottom of the screen. As soon as the application has been loaded, the SMT menu shown in Fig. 4.2-1 appears at the right of the screen¹. Details of all SMT commands are given in the next section.

If the drawing has a layer named "Floor1," it is automatically made the current layer as soon as the SMT is loaded. This layer is essential for accurate coverage prediction using the single-floor partition attenuation factor path loss model which is the default single floor model used by the SMT. If this layer does not exist in the drawing, the SMT displays a warning message (No "Floor1" layer present) on start-up.

¹ If the standard AutoCAD screen is not displayed, the user needs to invoke the "Preferences" sub-menu selection (under the "File" toolbar menu selection), toggle the screen menu selection, and save changes to the *acad.ini* file in the AutoCAD "Preferences" dialog box.

The user may now place a transceiver or interference source anywhere on the displayed floor plan by selecting the TRANSCVR or INTSRC command from the menu. When one of these commands is invoked for the first time, the SMT creates a new layer called "Icons" on which it draws all transceiver and interference source icons. The location coordinates of the transceivers and interferers (as well as the floor they are placed on) are stored in a transceiver/interferer linked list that is maintained in the Environment Description module, and not in the drawing itself.

After one or more transceivers have been placed, the user may invoke the DISPLAY or SELECT_1 commands to view the resulting coverage region. An example of this was shown in Fig. 1.5-1. The SMT calculates and displays two coverage contours for each transceiver. The outer contour, displayed in red, represents the threshold where the mean received signal level is approximately equal to the default SMT thresholds ($C/N = 18$ dB or $C/I = 10$ dB, whichever is lower), as calculated by the RF channel model equations. This contour is drawn on a specially created layer named "Ocntrf," where f is the number of the current floor. The boundary of the inner contour, displayed in green, represents the received signal threshold that is 10 dB *above* the outer boundary. This contour is also drawn on a specially created layer named "Icntrf." The reason for computing two separate layers is to assist the user in providing a safety margin when assessing overall building coverage. As in conventional cellular radio systems, this safety region could represent the *hand-off* region. The 10 dB difference may be modified by invoking the SMT command ICMARGIN at the command line.

As each contour is drawn, its interior region is highlighted with a hatched pattern. The density of this hatched pattern may be changed from its default of 15 by invoking the command HSIZE at the command line. It is important to note that increased density results in a reduction of processing speed, since AutoCAD tests each hatch pattern entity in determining the number of intervening partitions in all subsequent SMT calculations.

In computing coverage regions for a given floor, the SMT automatically considers all transceiver and interference sources that have been placed on any floor. Coverage contours are computed only for the floor that is currently visible. The active same-floor channel model equation is used if the transceiver under consideration is on the current floor. Otherwise, the active multifloor model is used.

AutoCAD places no constraints on the number of layers that can be present in a drawing. In theory, therefore, the SMT can accommodate a building with any number of floors. The number is limited only by the multifloor environment data available to the user and the amount of memory that is available to AutoCAD.

4.2. Site Modeling Tool Commands

Fig. 4.2-1 shows the custom screen menu that has been developed for the SMT. Except for ICMARGIN, HSIZE, and FLOORHT, this menu lists all SMT commands. These may be selected using the mouse after the SMT has been loaded into AutoCAD.

Note that the use of many standard AutoCAD commands, after the SMT has been loaded, modifies the screen menu entries (except the "SMT" heading). The SMT entries can be displayed once again by simply selecting this heading with a mouse click.

Each of the SMT commands is now discussed in detail.

4.2.1 Placement Commands

LOAD_DWG

Invoking this command opens the standard AutoCAD "Open File" dialog box. The user may then open any AutoCAD floor plan to be used with the SMT, provided, of course, that the drawing has been suitably modified as described in Section 3.1. This

<i>Category</i>	<i>Menu item</i> <i>(8 characters max)</i>	<i>Description</i>
	SMT	menu label
<i>placement commands</i>	LOAD_DWG	load floor plan from file
	SAVE_DWG	save floor plan to file
	TRANSCVR	place transceiver
	INTSRC	place interference sources
	MOVE	move trans. or intf. source
	DELETE	delete trans. or intf. source
<i>environment attributes</i>	TRANSPAR	select transceiver parameters
	ENVMNT	select building type
	MODEL	select propagation model
	PAF	partition attenuation factors
	FAF/Nmf	floor attn. factor / <i>n(multifloor)</i>
	INFO	trans. or intf. source parameters
<i>multifloor control</i>	UP_1_FL	move up one floor
	DWN_1_FL	move down one floor
	GO_TO_FL	specify floor to view
<i>program control</i>	DISPLAY	display all coverage contours
	CLEAR	clear all coverage contours
	SELECT_1	display single coverage contour
	CLEAR_1	clear selected coverage contour
	CNTR_RES	select coverage resolution
	CANCEL	cancel operation in progress

Fig. 4.2-1: The SMT screen menu. These abbreviations have been chosen because AutoCAD limits menu items to 8 characters.

command is the same as the AutoCAD command “Open” (under the toolbar menu labeled "File") under a different label.

SAVE_DWG

Invoking this command displays the standard AutoCAD "Drawing Modification" dialog box. The user may thus save or discard any changes made to the current floor plan drawing. This command is the same as the AutoCAD command “Save” (under the toolbar menu labeled "File").

TRANSCVR

This command allows the user to place any number of SMT transceivers on the current floor. The user can then view the coverage contour of any one or all of the transceivers by invoking the DISPLAY or SELECT_1 command, respectively. Transceivers on the current floor are displayed by a bold block outline (▣). Transceivers that have been placed on a different floor are visible in a block outline (□). As discussed in the description of the FLOORHT command below, each transceiver is given a default elevation of 0 m above the floor by the SMT.

INTSRC

Using this command, the user can place any number of single-tone interference sources on the current floor. Interference sources on the current floor are displayed by a bold block outline (◆). Interference sources that have been placed on a different floor are displayed in a block outline (◇). As discussed in the description of the FLOORHT command below, each interference source is given a default elevation of 0 m above the floor by the SMT.

MOVE

This command allows the user to reposition any transceiver or interference source previously placed onto the current floor by the TRANSCVR or INTSRC commands. The user is prompted (on the command line) to select the transceiver or interferer to move and then select the new location by a mouse click. For a transceiver being moved, its current coverage region, if already displayed, is first erased and the region around the new location is then automatically calculated and displayed. Transceivers or interferers on a floor other than the current one cannot be moved. An attempt to do so displays a warning via an SMT message dialog box.

DELETE

Any transceiver or interferer on the current floor can be deleted by invoking this command. The user is prompted (on the command line) to select the transceiver or interferer to delete, which he/she may then do by a mouse click. For a transceiver being deleted, its current coverage region, if already displayed, is also erased. Transceivers or interferers on a floor other than the current one cannot be deleted. An attempt to do so displays a warning via an SMT message dialog box.

4.2.2 Environment Attribute Commands

TRANSPAR

Invoking this screen command displays the SMT "Transceiver Parameters" dialog box. The user may then change any or all of the transceiver communication parameter values for all subsequent coverage region calculations. All transceivers on the floor plan, irrespective of whether they were placed before or after invoking this command, are assigned the communication parameters of the selected SMT transceiver type. The default

setting of the SMT is for the 915 MHz transceiver, and the associated parameter values have been listed in Table 3.1.2-1.

ENVMNT

Invoking this command displays the SMT "Environment Type" dialog box. The user may then select any environment type and thus set a value for the path loss exponent n . The user may also modify the default value of n itself. The default setting of the SMT is for an office environment with $n = 2.8$. However, it is important to realize that this value for n is used only for the same-floor distance-dependent path loss model. If a different path loss model is used, the value $n = 2$ overrides the value associated with the Environment Type.

MODEL

This command allows the user to select a specific model — one each for a single-floor and multifloor environment — according to which path loss will be determined. The default settings are the distance-dependent path loss model for the same-floor, and the floor attenuation factor path loss model for multifloor calculations.

Selecting the distance-dependent path loss model for the same and multifloor models voids the effect of the values of the partition-attenuation-factor and *FAF* (floor attenuation factor) respectively. Similarly, selecting the partition attenuation factor model or the *FAF* model voids the effect of the values of the environment type and n or $n(\text{multifloor})$ respectively.

PAF

Invoking this command displays the SMT "Partition Attenuation Factor" dialog box. The user may then set any value for the soft and concrete attenuation factors. These values are used only if the partition attenuation factor model is being used for the same

floor contour determination. The default values are 1.4 dB/partition and 2.4 dB/partition for soft and concrete partitions respectively.

FAF / Nmf

Invoking this command displays the SMT "Floor Attenuation Factor" dialog box if the floor attenuation factor model is the active multifloor model. If the distance-dependent multifloor path loss model is in effect, the "*n(multifloor)*" dialog box is displayed instead. The user may then set any values for these building parameters.

The default values used by the SMT for *n(multifloor)* and the *FAF* are listed in Table 3.2.4-1 and Table 3.2.4-2 respectively. It is important to note that the SMT uses the same values of *FAF* or *n(multifloor)* if the floor difference is equal to or greater than 5 or 3 floors respectively.

INFO

Upon invoking this command, the user is prompted to select a transceiver or interferer with a mouse click. The corresponding parameters are then displayed in a dialog box. For a transceiver, this information is simply its location coordinates on the floor plan. For an interferer, its current status (whether turned "on" or "off"), transmitting frequency, and power are also displayed and can be edited. The location coordinates of the transceiver or the interferer cannot be edited from this dialog box. To do so, the MOVE command (discussed above) must be invoked.

4.2.3 Multifloor Control Commands

UP_1_FL

Selecting this menu option moves the displayed floor up by one level for a multi-

story floor plan. If the user is currently on the highest floor of a drawing, invoking this selection displays an SMT message (Invalid floor) dialog box.

DWN_1_FL

Selecting this menu option moves the displayed floor down by one level for a multi-story floor plan. If the user is currently on the lowest floor of a drawing, invoking this selection displays an SMT message (Invalid floor) dialog box. Otherwise, this operation is similar to the UP_1_FL command.

GO_TO_FL

Invoking this command prompts the user to enter the number on the command line of the new floor to display. If the user enters an invalid floor number, SMT displays the SMT message (Invalid floor) dialog box.

When any multifloor control command is selected, the associated current floor layers are frozen, and the selected floor is made current. If the coverage region of a transceiver *on the current floor* is displayed, the regions are also frozen, but are automatically redisplayed if the user returns to this level at a later time. However, if the current floor is *not* the same as the transceiver floor, and its multifloor coverage region is displayed, then this region will be erased.

4.2.4 Program Control Commands

DISPLAY

This command causes the SMT to calculate and display all possible coverage regions on the current floor. For transceivers on the same floor, the active same-floor model is used to calculate path loss. For transceivers on different floors, the active

multifloor model is employed. If all transceivers are on different floors, and they provide no coverage on the current floor, the SMT displays a message to that effect.

Coverage is calculated and displayed starting with the most recently placed transceiver (irrespective of which floor it is placed on). If the coverage region of a transceiver is already on display, it is first erased and is then recalculated.

CLEAR

This command removes all displayed coverage regions from all floors.

SELECT_1

This command may be invoked to calculate and display the coverage region of a selected transceiver on the current floor. The user is prompted to select a transceiver with a mouse click.

CLEAR_1

This command clears the coverage region of a user-selected transceiver.

CNTR_RES

Invoking this command displays the SMT "Contour Resolution" dialog box. The user may then edit the distance resolution and/or the number of contour polygon points to be calculated. The default settings for the SMT are 1 m and 18 points for the distance resolution and number of points respectively.

CANCEL

Any AutoCAD command (including any of the above SMT commands) may be terminated by invoking this screen selection. Its effect is the same as entering ^C on the command line.

4.2.5 Additional Commands

The SMT also includes the following commands which may be invoked either from the command line or the SMT toolbar menu only.

ICMARGIN

This command allows the user to vary the threshold margin (in decibels) between the two contours. The current default SMT margin is 10 dB.

HSIZE

This command may be invoked to edit the density of the dotted contour hatch patterns. The default value of HSIZE in the SMT is 15. If no hatch pattern appears within a coverage region contour, the user needs to reduce this value of HSIZE. The recommended minimum value of HSIZE is 1.

FLOORHT

This command allows the user to vary the ceiling height of a multi-story building. The default SMT value for all ceiling heights in a building is set at 3 m. Different floors cannot be assigned different ceiling heights.

On any floor, all transceivers and interference sources are assigned an elevation of 0 m above that floor by the SMT. Thus, for example, if the ceiling height is 3m, the absolute elevation (z-position coordinate) of the transceivers or interferers placed on the first, second, and third floors will be 0 m, 3 m, and 6 m respectively. Changing the ceiling height value automatically scales the elevation of all transceivers and interference sources. Thus, if the new ceiling height is now set at 5m, the new z-coordinates of the above transceivers or interference sources will be set to 0 m, 5 m, and 10 m respectively.

If the ceiling height is set equal to or greater than 10 m, the SMT displays a warning message (Ceiling height too large. Results inaccurate.) before the calculation of *each* coverage region.

Chapter 5.

Site Modeling Tool Operational Examples

Now that all the salient features of the SMT have been described in the preceding chapters, several examples to illustrate the operation of the SMT are presented here. An important issue is that of the accuracy of the SMT in estimating the coverage regions, and this is discussed next. Although the SMT normally determines 18 boundary points for each coverage region, it is shown in this chapter that 36 boundary points are generally required for a good estimate, and no substantial advantage might be gained by further increasing this number of boundary points. Finally, the issue of operating speed of the SMT is also addressed.

5.1 Examples of Operation

To illustrate SMT operation, consider the floor plan that appears in Fig. 5.1-1. This is one floor of a building on the Virginia Tech campus, and contains several offices, classrooms, and storerooms. There are two elevator shafts and stairwells. This drawing was provided in AutoCAD form. Overall dimensions of the building as shown are 57 m by 91 m.

Instead of using this floor plan immediately, it is best if extraneous details are removed from consideration. Examples of these are arcs representing doors, lines representing stairs, and outside walkways. If the architect has placed such details on separate AutoCAD *layers*, it is a simple matter to ignore them during path loss computation. If they are not on separate layers, the user should remove them (or transfer them to new layers) for reasons of accuracy and efficiency.

Fig. 5.1-2 shows the same floor plan, but after the unnecessary details have been removed. In the figure, the user has initiated the SMT and has placed a transceiver near the center of the building. The resulting coverage region for this transceiver is indicated by two bold contours with a dotted fill pattern. The inner and outer contours represent "safe" and "marginal" coverage regions respectively, and are separated by a 5 dB margin in these examples. The partition attenuation factor path loss model has been used (Section 3.2.3), and 36 boundary points have been located on each contour.

Fig. 5.1-3 illustrates the effect of moving the transceiver by a small amount. By simply translating the transceiver to the corner of the original room, the shape of the coverage region is altered significantly. Fig. 5.1-4 demonstrates the effect of a single-tone interferer. The transceiver is in the same location as for Fig. 5.1-3. Notice that the coverage region opposite the interferer is unchanged, but the coverage near the interferer is altered dramatically.

Now assume that the user moves to the floor immediately above the one under consideration. The user places a transceiver on that floor, and returns to the initial floor. The coverage region for the second transceiver can then be displayed, as shown in Fig. 5.1-5. The nearly circular region results from the new transceiver, and illustrates the fact that the multifloor path loss models do not consider partitions individually. Notice that the interferer has affected the marginal coverage area.

Finally, a floor plan for a different building appears in Fig. 5.1-6. Three transceivers have been placed, and their coverage areas highlighted. After viewing these coverage areas, a system designer would adjust their locations and consider adding a fourth transceiver to obtain complete coverage.

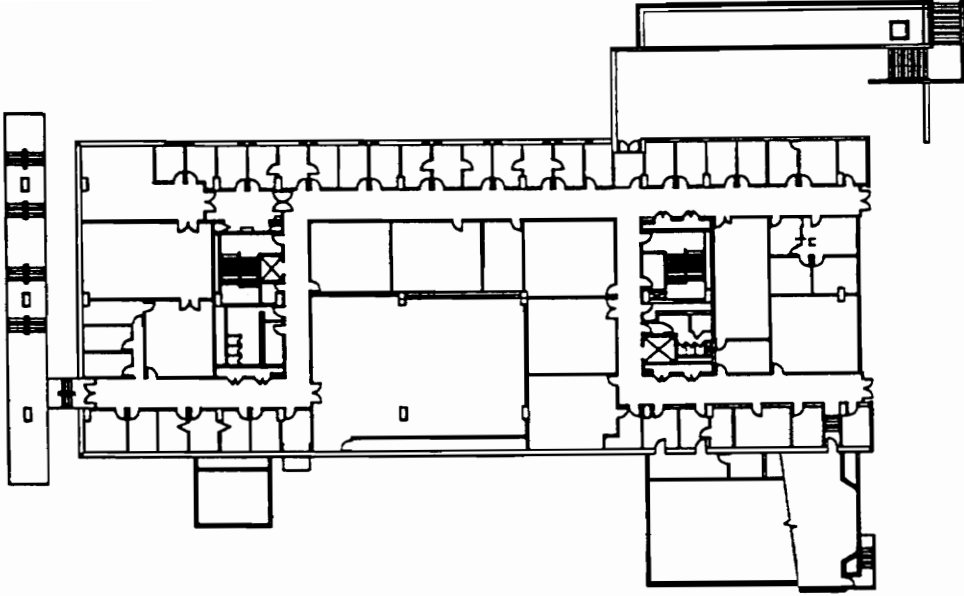


Fig. 5.1-1: Example floor plan. This is one floor of Whittemore Hall on the Virginia Tech campus. This drawing was generated directly from an AutoCAD file provided by the university's Facilities Planning and Construction department.

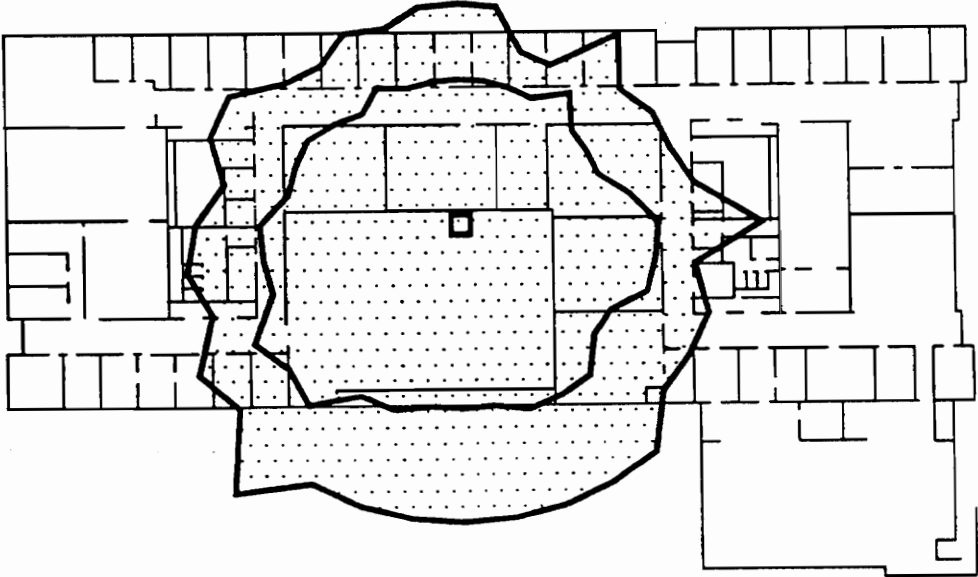


Fig. 5.1-2: Coverage contours for one transceiver. Unnecessary details have been removed from the drawing in the previous figure, and concrete partitions only are assumed. Notice that the coverage area is reduced near regions where many partitions are present. The drawing is more appealing when viewed in color on the PC's monitor.

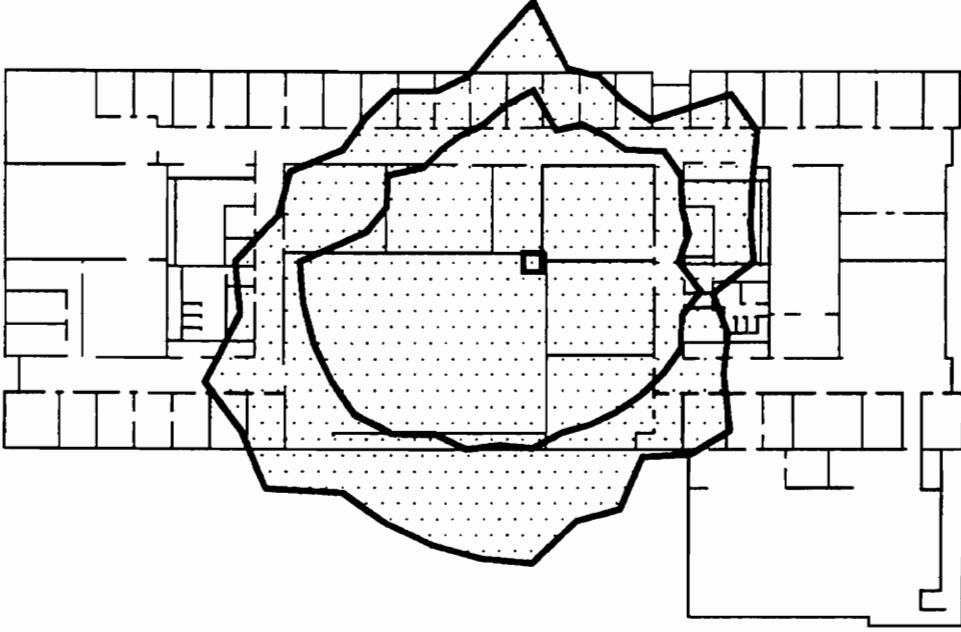


Fig. 5.1-3: Coverage contours for repositioned transceiver. The transceiver of the previous figure has been moved to the right by a small amount.

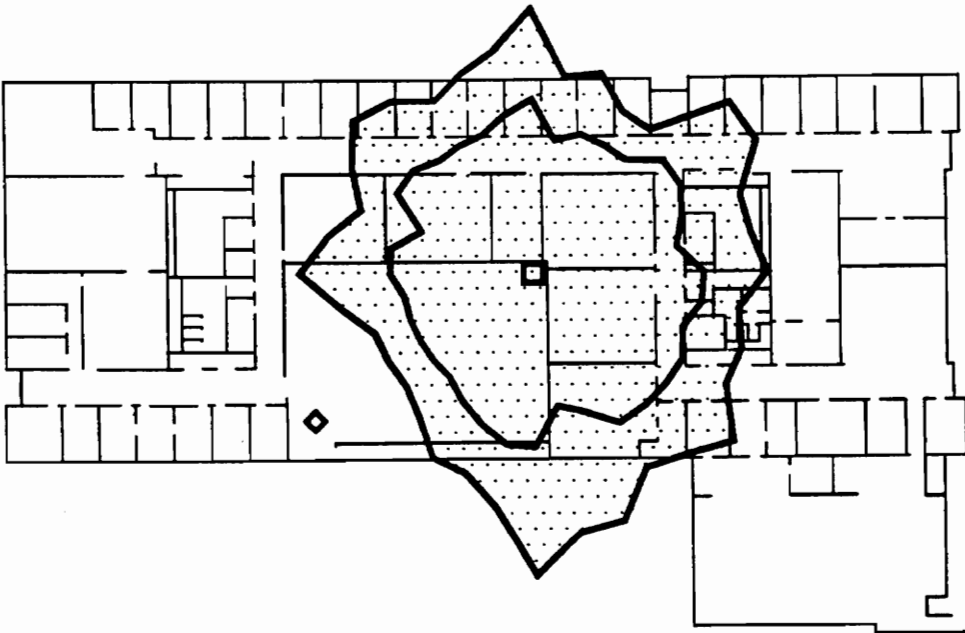


Fig. 5.1-4: Effect of single-tone interferer. The transceiver has not moved from its location in Fig. 5.1-3. The coverage area is changed considerably by the interference source.

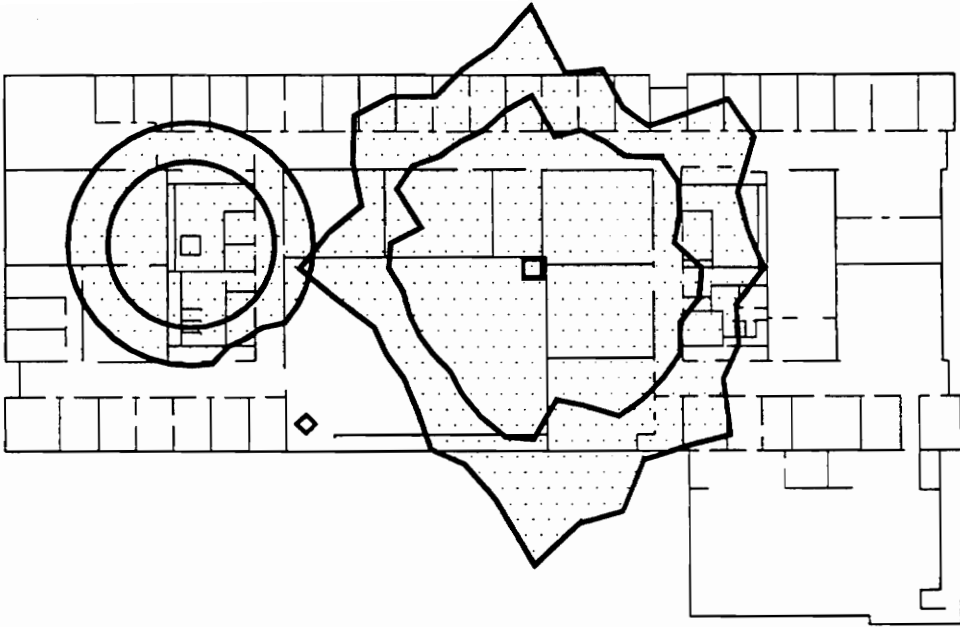


Fig. 5.1-5: Addition of coverage contours for transceiver on different floor. Transceivers not on the floor being viewed are distinguished by squares with thinner lines. The coverage area is nominally circular, but is perturbed here by the interference source.

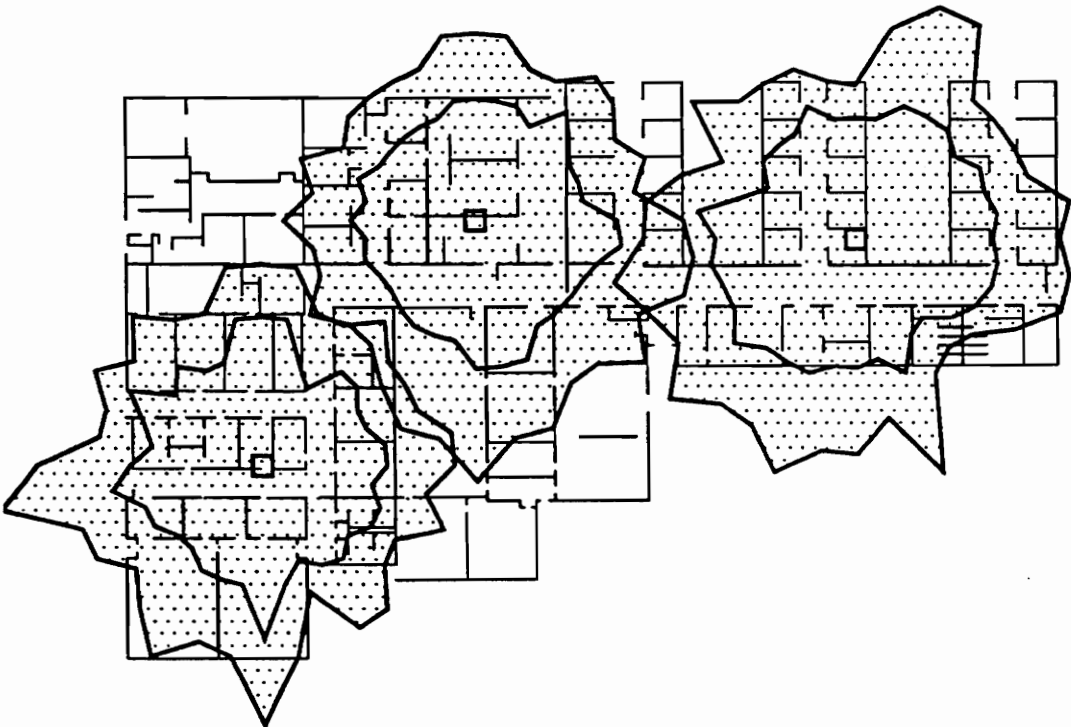


Fig. 5.1-6: Second example floor plan. This is one floor of Virginia Tech's Veterinary Medicine building. Three transceivers have been placed as a first attempt to provide complete floor coverage.

5.2 Accuracy Assessment

An important issue is that of the accuracy with which the SMT estimates coverage regions. It is not difficult to see that this accuracy is only as good as the models the SMT uses to predict the large-scale path loss. In Section 3.2.2., it was pointed out that a standard deviation σ that provides a quantitative measure of the accuracy of the models is very often quoted with a model or a set of measurements.

For the models used by the SMT described in Sections 3.2.3 and 3.2.4, a σ of 5.8 dB was reported for the entire data set from which the models were obtained in [Sei92b]. This implies that 67.7% of actual measurements would lie within ± 5.8 dB of the predicted mean path loss. For both the distance-dependent path loss models considered together, a σ of 16.3 dB has been reported. If only the single-floor distance-dependent path loss model is considered, the value of σ reduces to 12.9 dB. For the partition attenuation factor path loss model, a σ of only 4.1 dB has been reported. Estimates for σ for the floor attenuation factor model for a number of floor separations between the transmitter and receiver range from 1.5 to 7.0 dB in one building, and between 2.9 and 7.2 dB in another. All of these reported values for σ agree well with those reported by other researchers.

In addition to the measurements used to obtain the models in [Sei92b], the MPRG at Virginia Tech has made extensive path loss measurements in many other different types of buildings, including several on the Virginia Tech campus. In one experiment, measurements were made at frequencies of 1.3 GHz and 4.0 GHz on the second floor of Whittemore Hall [Sei92a]. The measurement locations for both these frequencies are shown in Figs. 5.2-1 and 5.2-2.

To perform a simple accuracy assessment of the partition attenuation factor path loss model, the path loss at all the above measurement locations was calculated using the

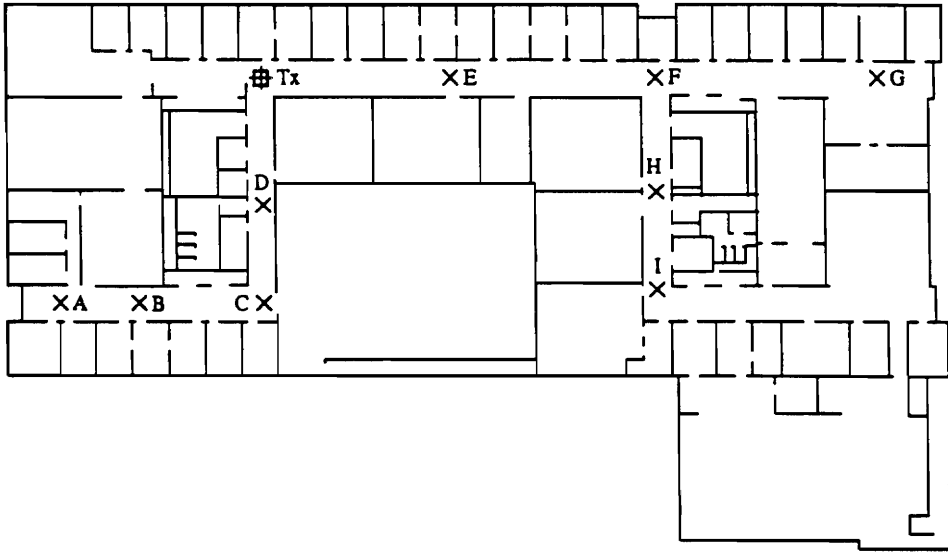


Fig. 5.2-1: Measurements at 1.3 GHz. The 9 locations labeled A through I represent receiver locations on the second floor of Whittemore Hall (Adapted from [Sei92a]).

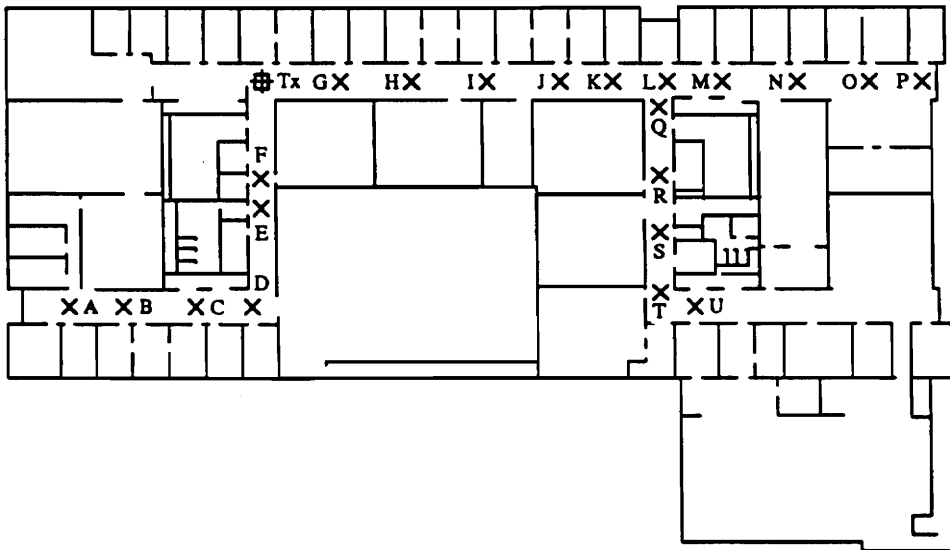


Fig. 5.2-2: Measurements at 4.0 GHz. The 21 locations labeled A through U represent receiver locations on the second floor of Whittemore Hall (Adapted from [Sei92a]).

Table 5.2-2: Measured and predicted path loss at 4.0 GHz on the second floor of Whittemore Hall (Adapted from [Sei92a]).

Measurement location	<i>T-R separation (m)</i>	<i>Number of intervening partitions</i>	<i>Measured path loss (dB)</i>	<i>Predicted path loss (dB)</i>
A	23.1	7	38.8	44.1
B	20.3	7	37.9	43.0
C	17.8	8	33.4	44.2
D	17.0	0	14.3	24.6
E	9.0	0	12.5	19.1
F	6.7	0	11.4	16.5
G	6.6	0	10.6	16.3
H	12.2	0	13.4	21.7
I	17.9	0	11.3	25.0
J	24.0	0	19.2	27.6
K	28.0	0	19.2	28.9
L	32.4	0	17.5	30.2
M	36.9	0	19.8	31.3
N	42.8	0	20.7	32.6
O	48.5	0	22.7	33.7
P	52.8	0	27.6	34.5
Q	31.7	4	29.9	39.6
R	32.3	5	38.3	42.2
S	33.5	7	43.8	47.3
T	35.3	5	47.6	43.0
U	38.3	5	56.0	43.7

A better and more valid assessment might be made by considering only those locations at both frequencies where the number of intervening partitions is at least one.

These results are summarized below:

- 1) At 1.3 GHz: Using 4 locations, $\sigma = 5.6$ dB.
 Error < 10 dB at 3 of 4 locations.
- 2) At 4.0 GHz: Using 8 locations, $\sigma = 7.6$ dB.
 Error < 10 dB at 6 of 8 locations.
- 3) For this entire data set: Using all 14 locations, $\sigma = 7.0$ dB.
 Error < 10 dB at 9 of 12 locations.

All the values of σ calculated above agree well with published results.

5.3 The Effect of Contour Resolution

In this section, we investigate the issue of increasing contour resolution on the shape of coverage regions. The effective contour resolution may be varied by changing either or both the distance and angular resolutions as described in Section 4.2.4.

The SMT always averages the last two distances determined for the coverage region along each radial line considered from the transceiver (see Section 3.4). The coverage boundary at each boundary point is therefore accurate to within half the selected distance resolution as predicted by the path loss models. Using (3.2) with $n = 2.0$ and a transmitter-receiver separation of $d = 10$ m, a distance resolution of 1 m (i.e., a distance resolution error of 0.5 m) translates into a signal strength prediction error of less than 0.5 dB. At a transmitter-receiver separation of 100 m, this error is a miniscule 0.04 dB. Clearly, the error introduced on account of the quantization of the distance resolution is far smaller than the standard deviation σ of the path loss model, and may therefore be safely disregarded.

The question of angular resolution is more important and can result in dramatic differences in the shape of the obtained coverage regions. Figs. 5.3-1 to 5.3-5 show the coverage region obtained for a transceiver located in the hallway of the same floor plan shown earlier. The same communication parameters and distance resolution but different angular resolutions were used to obtain these figures. In Fig. 5.3-1, only 9 boundary points were determined. It will soon be apparent that a resolution of this order falls far short of accurately depicting coverage regions. In Fig. 5.3-2, 18 boundary points have been determined. This resolution presents a good first approximation of the coverage region.

In Figs. 5.3-3 to 5.3-5, 36, 72, and 180 boundary points respectively have been determined and displayed. Fig. 5.3-5 looks very impressive, and one might easily be influenced to use a very large number of boundary points. Indeed, certain features such as the spikes generated on account of the longer unobstructed propagation of the radio energy along the hallways are obvious. However, almost all the other fine features along the boundary at such a high resolution occur due to the absence of doors in the floor plans. It is possible that these spikes might be obtained in practice if the doors were open, or absent entirely. However, the influence of doors has not been characterized in the path loss models, and such a fine coverage region is, infact, somewhat misleading as predicted by the propagation models given.

Figs. 5.3-3 and 5.3-4 are very good estimates of the shapes of the coverage regions. The latter selection is certainly preferable, but if we consider the trade-off between speed and accuracy of the SMT for the calculation of a large number of coverage regions (as might be required for optimal transceiver placement), the former resolution of 36 boundary points is actually a better choice. All the important features, including the spikes along the hallways, are visible in Fig. 5.3-3. Another factor in favor of this choice of angular resolution is that the influence of log-normal shadowing will, in any case, modify the coverage region shape in practice, and obviate the effect of higher resolution selections.

Thus, although the calculation of 36 boundary points appears to be a very good choice, the SMT calculates only 18 boundary points as a default. However, this choice was made solely on the basis of attempting to provide the user with a reasonably quick and good first approximation of the coverage region. The user is free to increase this resolution and experiment with the shape of the coverage regions as necessary.

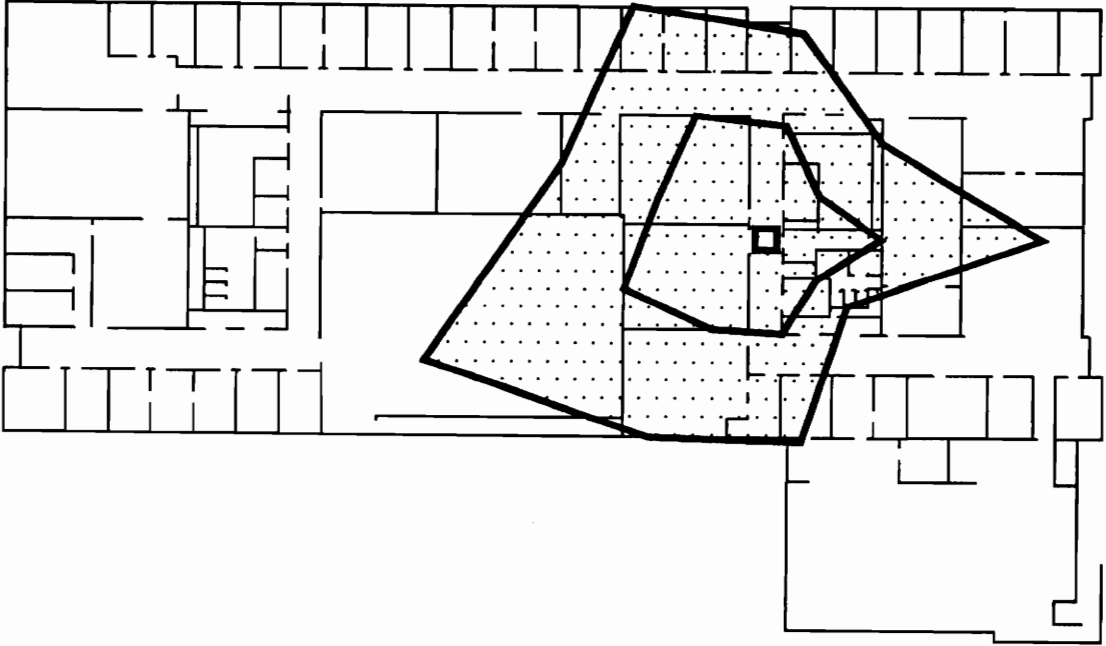


Fig. 5.3-1: Coverage region for a transceiver obtained by determining only 9 boundary points.

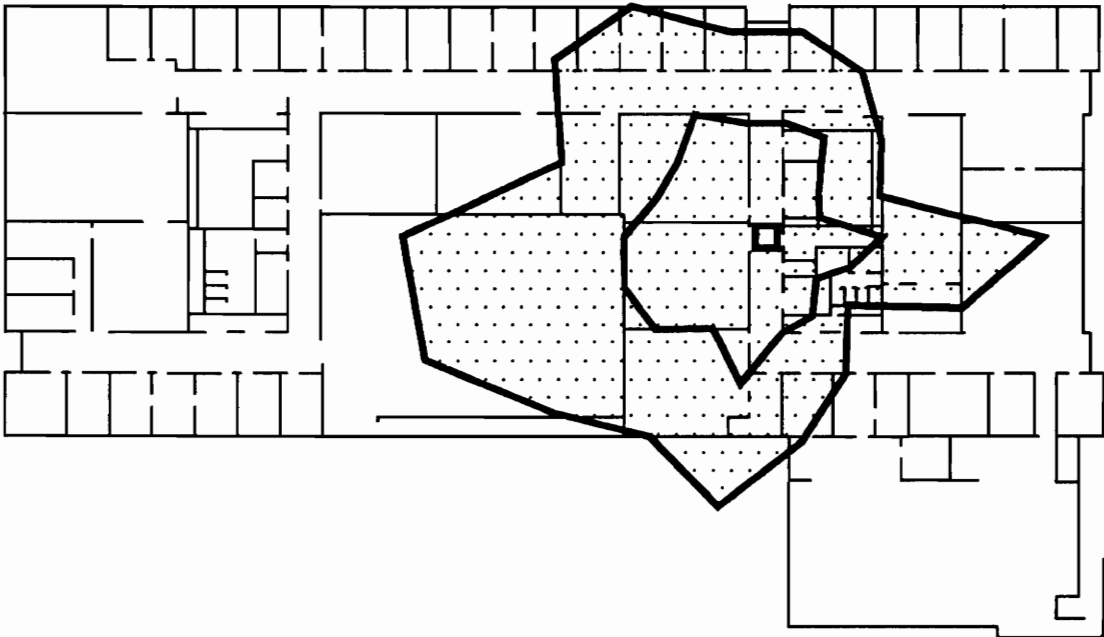


Fig. 5.3-2: Coverage region for the same transceiver obtained by determining 18 boundary points. This angular resolution provides a reasonably good first order estimate of the coverage region.

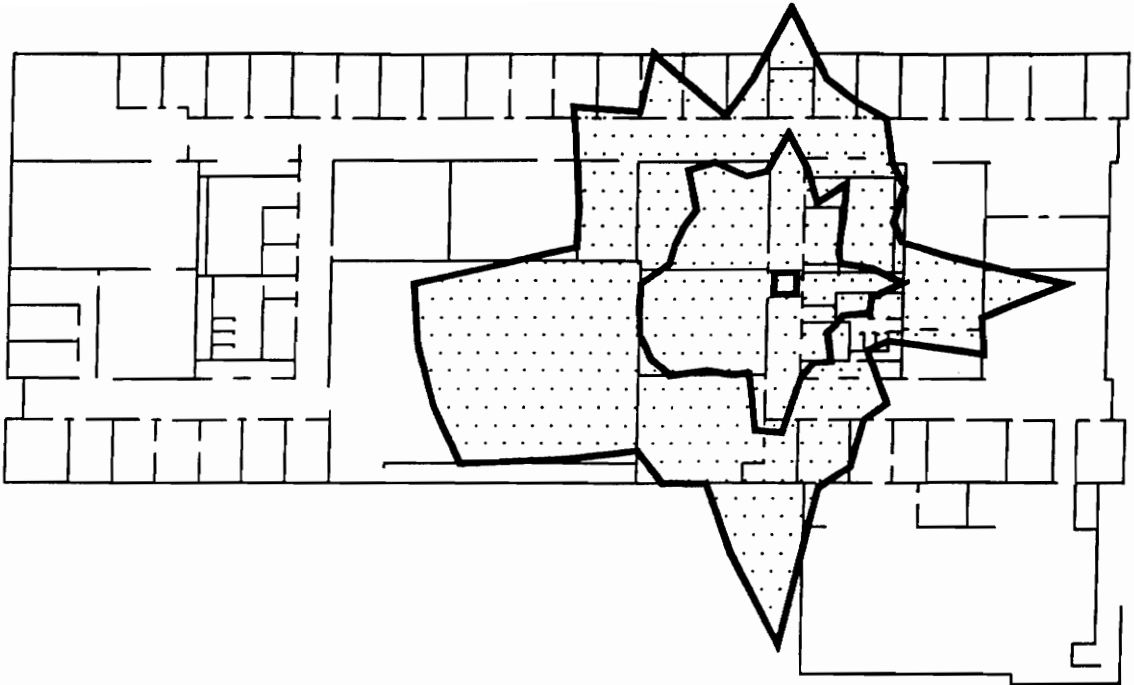


Fig. 5.3-3: Coverage region obtained by determining 36 boundary points. This angular resolution is most often sufficient to provide a very good working estimate of the coverage region.

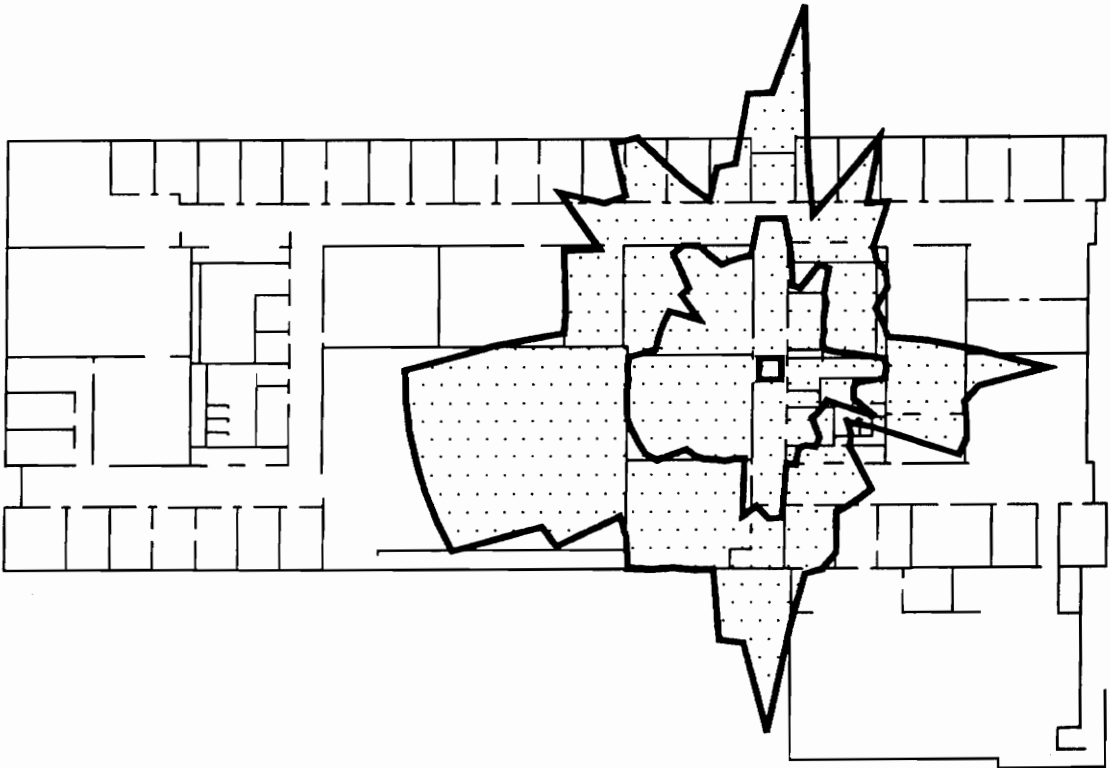


Fig. 5.3-4: Coverage region obtained by determining 72 boundary points. This angular resolution may be used for higher resolution in highly cluttered areas if 36 boundary points do not suffice.

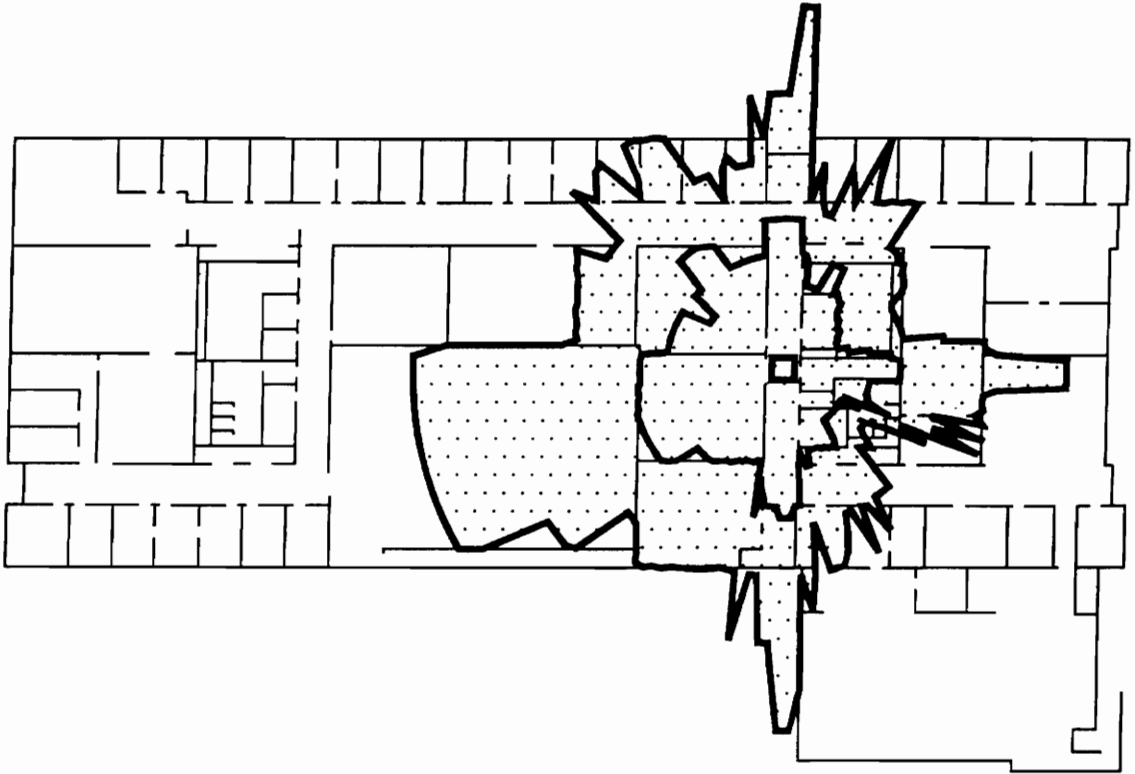


Fig. 5.3-5: Coverage region obtained by determining 180 boundary points. This angular resolution, although very impressive, might actually be a little inaccurate.

5.4 Operating Speed of the Site Modeling Tool

5.4.1 Examples of Operating Speed

Another important issue is that of the operating speed of the SMT — the time it takes to calculate the coverage region boundary points. In this section, we investigate this issue by providing an approximate quantitative analysis.

Tables 5.4.1-1 to 5.4.1-4 list some representative times (t_{calc}) that were measured for calculating the coverage region of a transceiver only, as well as for the combination of one transceiver and an interferer using different path loss models and contour resolutions. The computing platform used was an IBM-compatible 486 DX-2 PC operating at 66 MHz. It is important to note that the calculation times tabulated are not exact, but are only meant to be indicative of the order of the expected values of t_{calc} . Furthermore, these

values will be different if the SMT is run on a different hardware platform. However, a method to compare relative coverage calculation times that is independent of the hardware platform is also presented.

For the values of t_{calc} listed in Table 5.4.1-1, a single transceiver located as shown in Fig. 5.1-3 was used along with the partition attenuation factor path loss model. The transceiver parameter values, and therefore, the coverage region shown, were also very similar. The t_{calc} values shown are also plotted as a function of the number of boundary points $N_{bp} = \|P\|$ determined for different distance resolutions (d_{res}) in Fig. 5.4.1-1. From this figure, we see that doubling N_{bp} (equivalent to halving the angular resolution) approximately doubles the value of t_{calc} . This is intuitive, since the SMT will take twice as long to calculate twice the number of boundary points. Halving d_{res} increases t_{calc} by a factor of 50%, since the SMT now has to test communication feasibility at a larger number of points.

To obtain the t_{calc} values listed in Table 5.4.1-2, the same floor distance-dependent path loss model was used instead of the partition attenuation factor path loss model. The value of n used was 2.5 so as to provide a coverage region comparable in terms of coverage area to that shown in Fig. 5.1-3. In this case however, a very large nu-

Table 5.4.1-1: Coverage region calculation times as a function of distance and angular resolutions, for a single transceiver using the partition attenuation factor path loss model. The observed times will vary with the complexity of the floor plan, as well as the values of the communication parameters.

Number of boundary points (N_{bp})	Coverage region calculation times (t_{calc}) in seconds for distance resolution (d_{res}) =			
	4.0 m	2.0 m	1.0 m	0.5 m
9	4	6.5	9	15
18	7.5	11.5	16	27
36	14.5	21	31	53
72	29	41	63	107
144	59	80	127	215

Table 5.4.1-2: Coverage region calculation times as a function of distance and angular resolutions, for a single transceiver using the same floor distance-dependent path loss model. The computation times are independent of floor plan complexity.

<i>Number of boundary points</i> (N_{bp})	<i>Coverage region calculation times (t_{calc}) in seconds for distance resolution (d_{res}) =</i>			
	<i>4.0 m</i>	<i>2.0 m</i>	<i>1.0 m</i>	<i>0.5 m</i>
180	7	7	7	8
360	14	14	15	15.5
720	28	29	30	31

Table 5.4.1-3: Coverage region calculation times as a function of distance and angular resolutions, for a single transceiver and interferer using the partition attenuation factor path loss model.

<i>Number of boundary points</i> (N_{bp})	<i>Coverage region calculation times (t_{calc}) in seconds for distance resolution (d_{res}) =</i>	
	<i>2.0 m</i>	<i>1.0 m</i>
9	10	15
18	19	29
36	38	58
72	76	115
144	157	172

Table 5.4.1-4: Coverage region calculation times as a function of distance and angular resolutions, for a single transceiver and interferer using the same floor distance-dependent path loss model.

<i>Number of boundary points</i> (N_{bp})	<i>Coverage region calculation times (t_{calc}) in seconds for distance resolution (d_{res}) =</i>	
	<i>2.0 m</i>	<i>1.0 m</i>
180	7.5	8
360	15	16
720	30	31

number of boundary points were determined to provide measurable and more accurate estimates for t_{calc} . We observe that the values for t_{calc} listed in Table 5.4.1-2 remain almost unchanged for different values of d_{res} . Doubling N_{bp} does, however, double t_{calc} as before.

Tables 5.4.1-3 and 5.4.1-4 are similar to Tables 5.4.1-1 and 5.4.1-2 respectively, except that these values for t_{calc} were measured by placing an interference source at the location shown in Fig. 5.1-4. The nature of the dependence of t_{calc} on N_{bp} and d_{res} is the same as it was for only a single transceiver in the preceding case, but the addition of the interferer now approximately doubles the values of t_{calc} , as shown in Fig. 5.4.1-2. This can be attributed to the fact that the SMT now has to determine the number of partitions between the point under test for communication feasibility as well as the interferer, in addition to the transceiver. As we shall soon see, this is a very important point that effectively determines the operating speed of the SMT.

A striking point that is obvious from a comparison of Table 5.4.1-2 with Table 5.4.1-1 and of Table 5.4.1-4 with Table 5.4.1-3 is that the values of t_{calc} are *much* smaller when the distance-dependent model is used. Under the valid assumption that the number of points where communication feasibility is tested is of the same order for both the path loss models, we can easily see that the slower times for the partition attenuation factor path loss model can be attributed to the additional computation of the number of intervening partitions by AutoCAD at each receiving point tested. For most of the values tabulated in Tables 5.4.1-1 and 5.4.1-3, *well over 90%* of the calculation time is consumed by this computation. Several techniques were attempted to increase AutoCAD's speed in doing this calculation, but apparently AutoCAD has already implemented most of the ideas internally. The determination of the number of intervening partitions thus forms the bottleneck of the attempt to increase the SMT's operating speed.

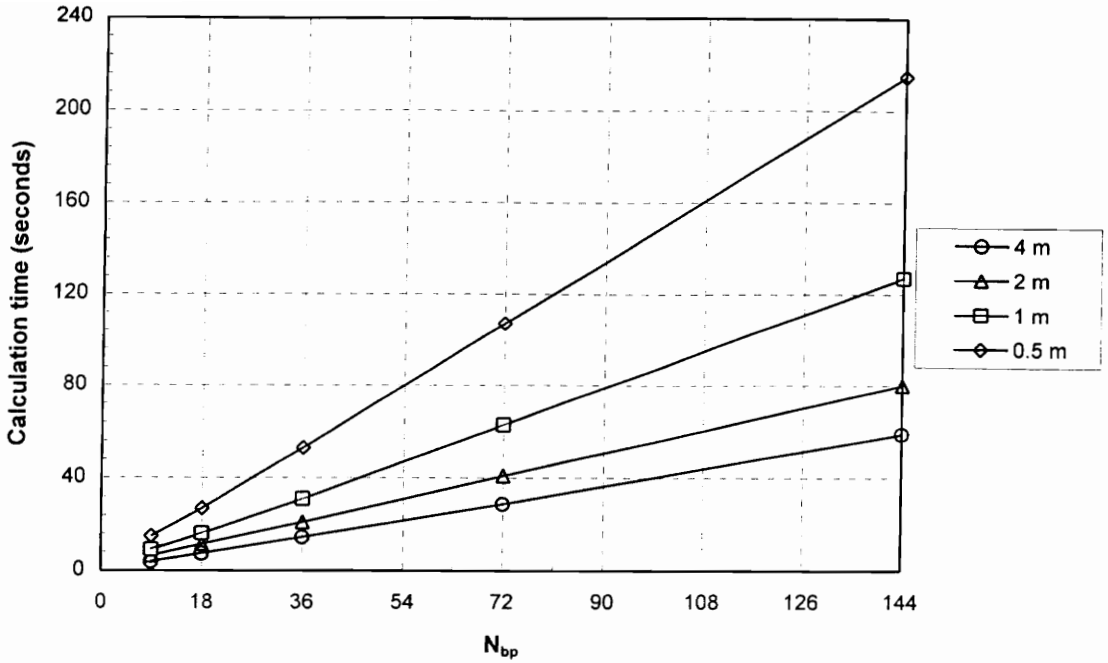


Fig. 5.4.1-1: Relative plots of the time taken to calculate a coverage region as a function of the number of boundary points for different values of d_{rev} . The transceiver was placed at the location shown in Fig. 5.1-3.

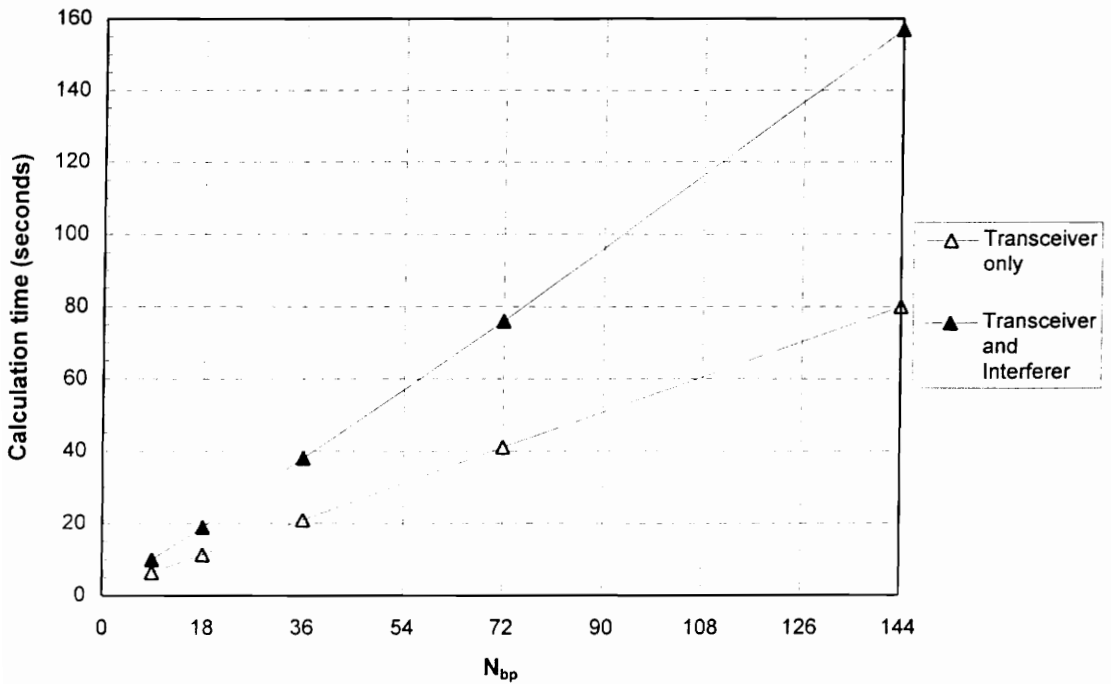


Fig. 5.4.1-2: Relative plots of the time taken to calculate a coverage region for a transceiver only, as well as a transceiver and an interferer, as a function of the

To summarize this section, we note that operating speed is not an issue when the distance-dependent path loss model is used, and t_{calc} is of the order of 2-5 seconds for practical contour resolution values. For the slower but more accurate partition attenuation factor path loss model, fairly accurate coverage regions for only a single transceiver can be viewed in 15-30 seconds. The inclusion of one or two interferers will still allow determination of a coverage region in about 60 seconds or less.

5.4.2 Estimating Coverage Region Calculation Times

Using the values listed in Tables 5.4.1-1 and 5.4.1-3 above, an empirical relation was derived which allows us to estimate relative values (t_{calc}^*) of t_{calc} for a coverage region in terms of the number of interferers (I), N_{bp} , and d_{res} for use with the partition attenuation factor path loss model. This can be written as

$$t_{calc}^* \propto (I + 1) \times \left(\frac{N_{bp}}{36} \right) \times \left(\frac{1}{1.5^{\log_2(d_{res})}} \right). \quad (5.1)$$

This estimate of t_{calc}^* is *relative* to the time required to calculate a reference coverage region with $N_{bp} = 36$ and $d_{res} = 1.0$ m. The exact value of t_{calc} will depend on the particular computer on which the SMT is run. The hardware configuration used to measure the values listed above takes approximately 30 seconds to calculate the reference contour. Hence, we may modify (5.1) only for this system as

$$t_{calc} \approx 30 \times t_{calc}^* \quad [\text{seconds}].$$

Chapter 6. The Effect of Interference Sources

6.1 Introduction

As illustrated in Section 5.1, interferers can have a dramatic effect on the shape and size of a transceiver's coverage region. Equations (3.2) and (3.9) - (3.17) yield additional insight into this effect. In this chapter, we attempt to quantify the effect of interferers in terms of the size and shape of the coverage regions. Partition losses are ignored, and the distance-dependent path loss model (3.2) is used for analysis. With this model, the coverage regions of influence of the transceiver and interferer are both circular. This chapter will demonstrate that the effect of interferers can be modeled surprisingly easily by looking at the intersection between two circles of various diameters and relative positions. The analysis is further simplified by considering the interaction between a single transceiver and a single interferer. It is also assumed that the interferer operates at the same frequency as the transceiver (i.e., the transceiver receive filter characteristics are ignored), and that the signal propagation characteristics are the same. Furthermore, it is assumed that, at any point, U is smaller than W (see Section 3.3.2). Since U will always therefore violate (3.18) before W will, it defines the limit of the transceivers region of influence, and we can completely ignore W . If W were greater than U , we could simply substitute W for U at all steps in the following analysis.

6.2 The Simplified C/N and C/I Contours

Figs. 6.2-1 and 6.2-2 are the signal level and contour plots of U (equation (3.14)) and V (equation (3.15)) respectively. These, and all the subsequent plots have been obtained using the parameter values listed in Table 6.2-1 below.

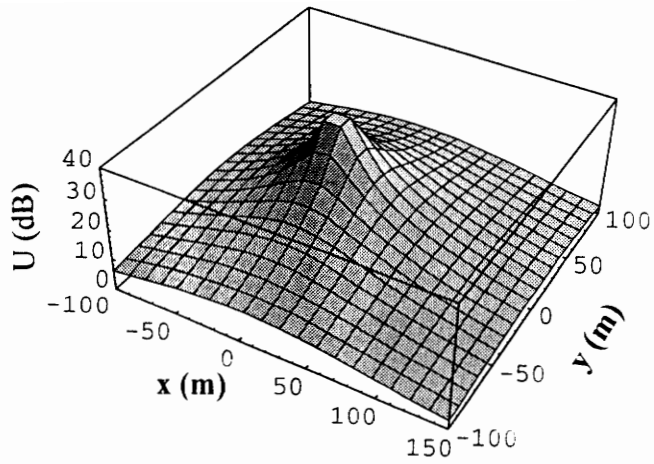


Fig. 6.2-1(a).

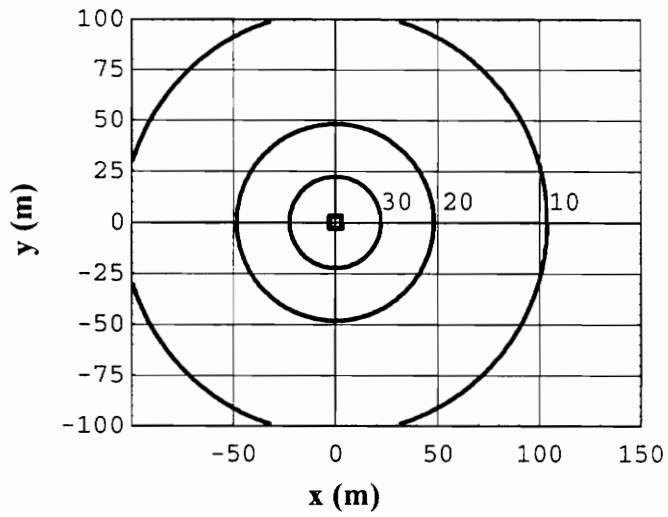


Fig. 6.2-1(b).

Fig. 6.2-1: (a) Signal level and (b) contour plots of U in dB. The transceiver is located at the origin.

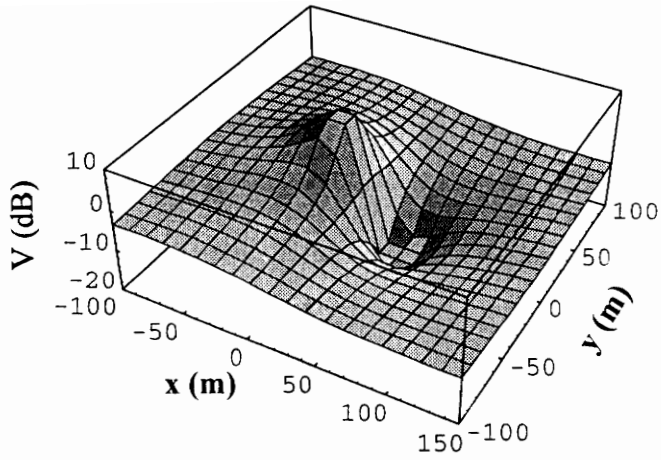


Fig. 6.2-2(a).

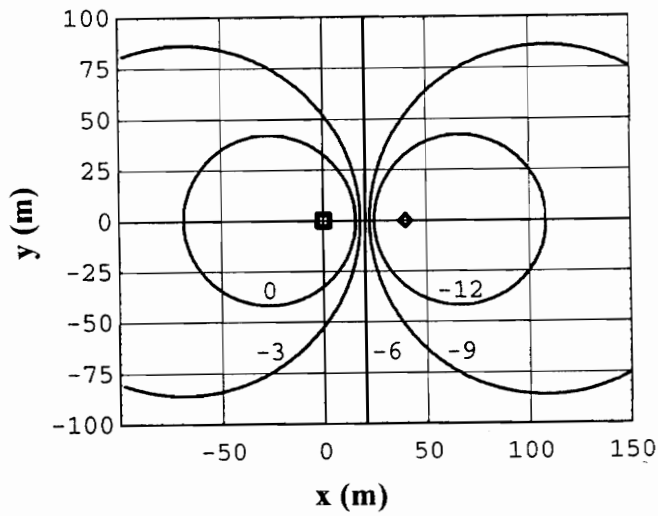


Fig. 6.2-2(b).

Fig. 6.2-2: (a) Signal level and (b) contour plots of V in dB. The transceiver is located at the origin and the interferer is located at $(40,0)$. The positive and negative peaks in V arise at the location of the transceiver and interferer respectively.

Table 6.2-1: Values for communication parameters used in Figs. 6.2-1 to 6.5-2.

<i>Variable</i>	<i>Value</i>	<i>Units</i>
n	3.0	-
f	900	MHz
$PL(d_0)$	31.5	dB
P_t	24	dBm
P_i	20	dBm
N	-126	dBm
$(C/N)_{\min}$	18	dB
$(C/I)_{\min}$	10	dB

Without loss of generality, it is assumed that the transceiver is located at the origin of the Cartesian coordinate system and the interferer is located some distance away from the transceiver along the positive x axis at $(x_i, 0)$ on the same floor. In all the following figures, $x_i = 40$ m. The positive and negative peaks in V arise because of the peaks in P_t and P_i at the positions of the transceiver and the interferer.

Consider a particular contour of (3.14), determined by an arbitrary threshold $U = u_t$. Substituting (3.2), (3.9), and (3.10) in (3.14) and simplifying, we obtain

$$U = u_t = \left(\frac{C}{N} \right) - \left(\frac{C}{N} \right)_{\min} \quad [\text{dB}]$$

$$u_t = \left[P_t - \overline{PL}(d_0) - 10n \log_{10}(d_t/d_0) \right] - \left[P_n + P_e \right] - (C/N)_{\min} \quad [\text{dB}]$$

$$\log_{10}(d_t/d_0) = \left[\frac{P_t - \overline{PL}(d_0) - (P_n + P_e) - u_t - (C/N)_{\min}}{10n} \right]$$

$$\text{Therefore, } d_t^2 = x^2 + y^2 = d_0^2 10^{\left[\frac{P_t - \overline{PL}(d_0) - (P_n + P_e) - u_t - (C/N)_{\min}}{5n} \right]} = K_1^2 \quad (\text{a constant})$$

The contours which satisfy $U = u_t$ are therefore circular (as expected), centered at the transceiver, and with radius K_1 .

The contours determined by an arbitrary threshold $V = v_t$ are also circular, although this is not immediately apparent. Beginning with (3.15), and substituting (3.2), (3.9), and (3.11), we obtain

$$V = v_t = \left(\frac{C}{I}\right) - \left(\frac{C}{I}\right)_{\min} \quad [\text{dB}]$$

$$v_t = \left[P_t - \overline{PL}(d_0) - 10n \log_{10}(d_t/d_0) \right] - \left[P_i - \overline{PL}(d_0) - 10n \log_{10}(d_t/d_0) \right] - (C/I)_{\min} \quad [\text{dB}]$$

$$\log_{10}(d_t/d_i) = \left[\frac{P_t - P_i - (C/I)_{\min} - v_t}{10n} \right]$$

Substituting $d_t^2 = x^2 + y^2$ and $d_i^2 = (x - x_i)^2 + y^2$, we have

$$x^2 + y^2 = [(x - x_i)^2 + y^2] 10^{\left[\frac{P_t - P_i - (C/I)_{\min} - v_t}{5n} \right]} \quad (6.1)$$

Setting $K_2^2 = 10^{\left[\frac{P_t - P_i - (C/I)_{\min} - v_t}{5n} \right]}$, (6.1) can be rewritten as

$$\left(x - \frac{x_i K_2^2}{K_2^2 - 1} \right)^2 + y^2 = \left(\frac{x_i K_2}{K_2^2 - 1} \right)^2,$$

which represents a circle with center $(x_i K_2^2 / (K_2^2 - 1), 0)$ and radius $x_i K_2 / (K_2^2 - 1)$.

6.3 The Effect of Interferers on Coverage Regions

Let the thresholds u_t and v_t determine regions S_u and S_v as follows:

$$S_u = \{ (x, y) \mid U(x, y) \geq u_t \}$$

$$S_v = \{ (x, y) \mid V(x, y) \geq v_t \}$$

The final coverage region in which communication is possible is the intersection $S = S_u \cap S_v$ introduced in Section 2.2. As demonstrated below, different choices for u_t and v_t result in dramatically different coverage regions.

First consider Fig. 6.3-1, which contains plots of U and V as a function of x . For the choice of v_t shown, an infinite number of coverage regions are possible based on the choice of u_t . The region *outside* the circle defined by $V = v_t$ represents the region S_v where $V > v_t$. Five different selections, u_{t1}, \dots, u_{t5} , are also illustrated in Fig. 6.3-1. Fig. 6.3-2 shows the coverage regions which result. For large u_t thresholds, S_u is completely contained in S_v as illustrated in Fig. 6.3-2(a). When u_t is reduced to u_{t2} (as shown in Fig. 6.3-2(b)), the contours $U = u_t$ and $V = v_t$ touch at a single point. For $u_t < u_{t2}$, the region $S_u \cap S_v$ depends on the intersection of two circular regions (Fig. 6.3-2(c)). For $u_t \leq u_{t4}$, S_u completely encloses the "interference zone" \bar{S}_v (Fig. 6.3-2(d-e)).

Similarly, Fig. 6.3-3 shows another selection of v_t , and five different selections u_{t6}, \dots, u_{t10} . The resulting coverage regions are illustrated in Fig. 6.3-4. For large u_t thresholds, S_u is completely contained in S_v . When u_t is reduced to u_{t7} (Fig. 6.3-4(b)), the contours $U = u_t$ and $V = v_t$ touch at a single point. For $u_t < u_{t7}$, the region $S_u \cap S_v$ once again depends on the intersection of two circular regions (Fig. 6.3-4(c)). For $u_t \leq u_{t9}$, S_u completely encloses S_v , and the coverage region can be given only by S_v (Fig. 6.3-4(d-e)).

Fig. 6.3-5 shows one last selection of v_t . For this condition, the region S_v is given by the entire left hand side plane bounded by the straight line $x = x_i/2$. Fig. 6.3-5 also shows three different selections u_{t11}, \dots, u_{t13} . For large u_t ($\geq u_{t12}$), S_u is completely contained within S_v . For smaller u_t ($< u_{t13}$), the coverage region is given by $S_u \cap S_v$ (Fig. 6.3-6(c)).

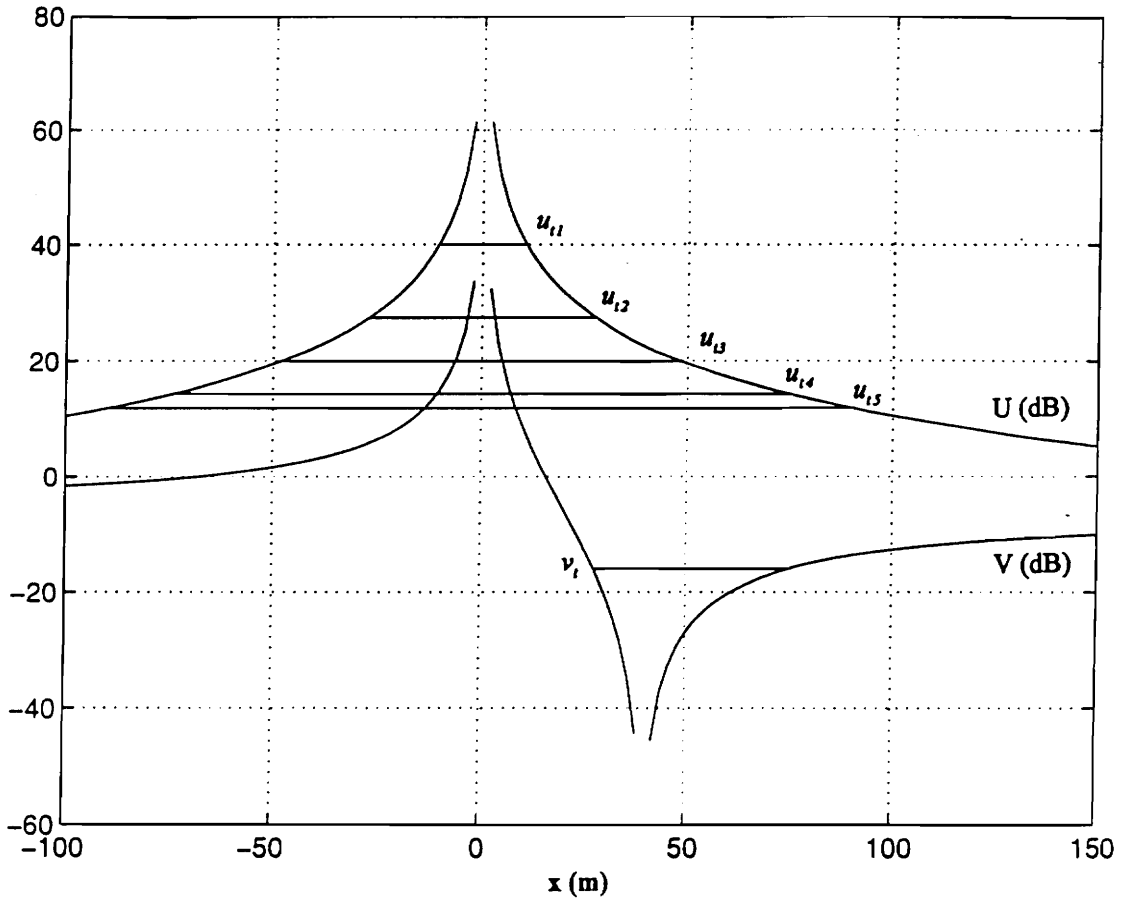


Fig. 6.3-1: Plots of U and V as a function of x . Several threshold values of $U = u_{t,1}, \dots, u_{t,5}$ and $V = v_t$ are indicated, as described in Section 6.3.

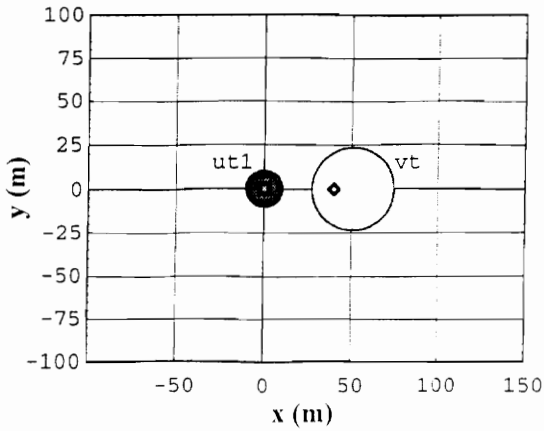


Fig. 6.3-2(a).

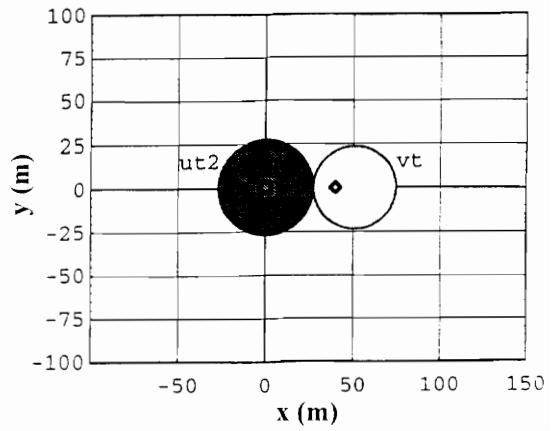


Fig. 6.3-2(b).

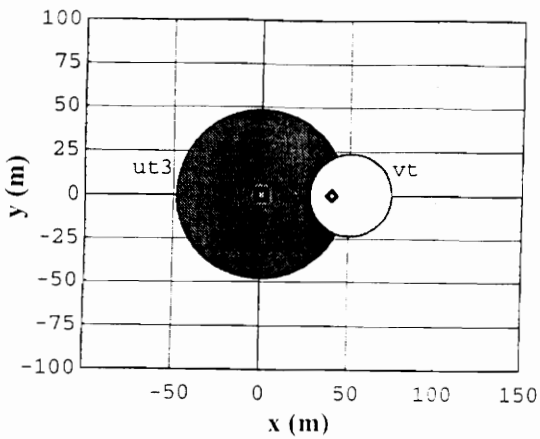


Fig. 6.3-2(c).

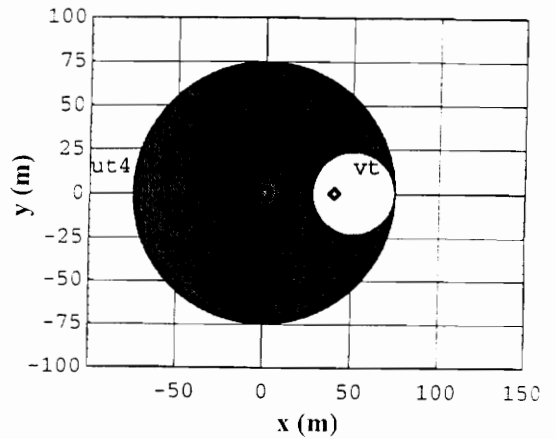


Fig. 6.3-2(d).

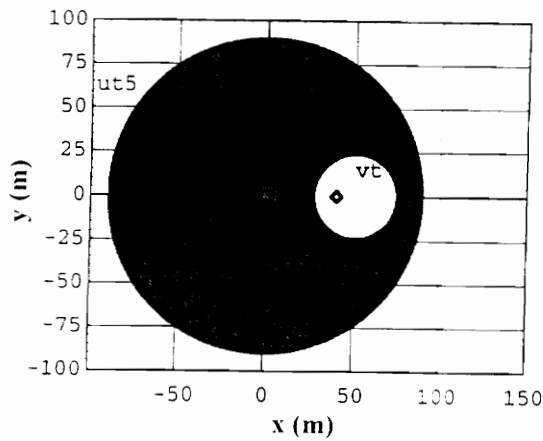


Fig. 6.3-2(e).

Fig. 6.3-2: The dark shaded areas are the coverage regions resulting from the selected values of u_i and v_i in Fig. 6.3-1. Note that S_u is inside the circle $U = u_i$, whereas S_v is outside the circle $V = v_i$.

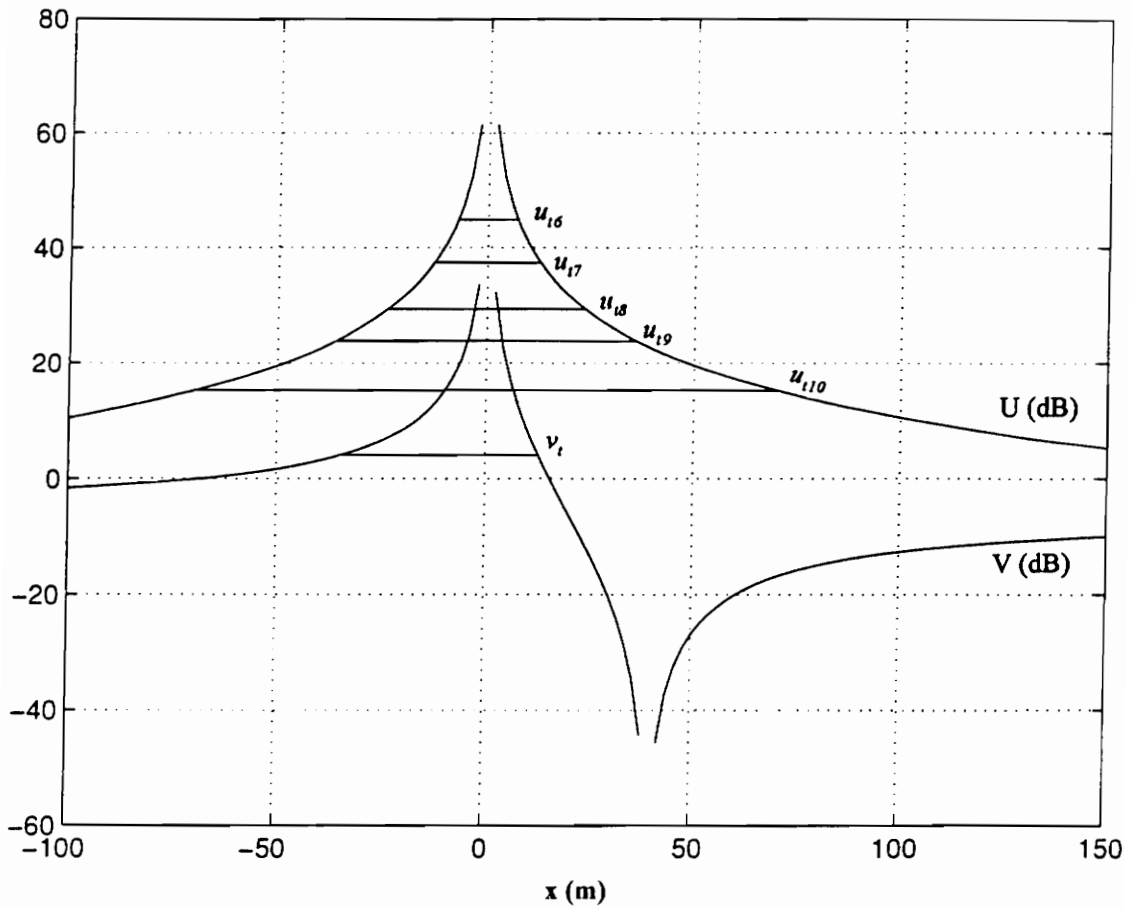


Fig. 6.3-3: Plots of U and V as a function of x . New threshold values of $U = u_{i6}, \dots, u_{i10}$ and $V = v_i$ are shown.

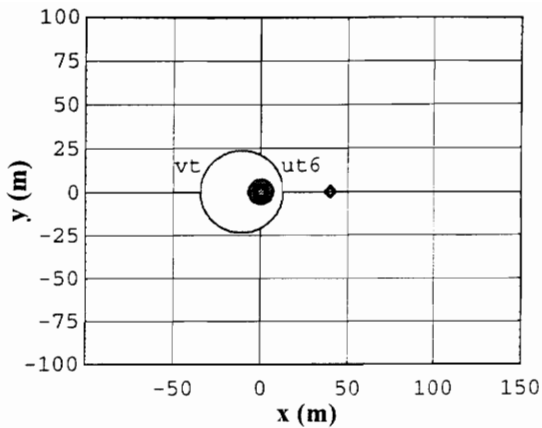


Fig. 6.3-4(a).

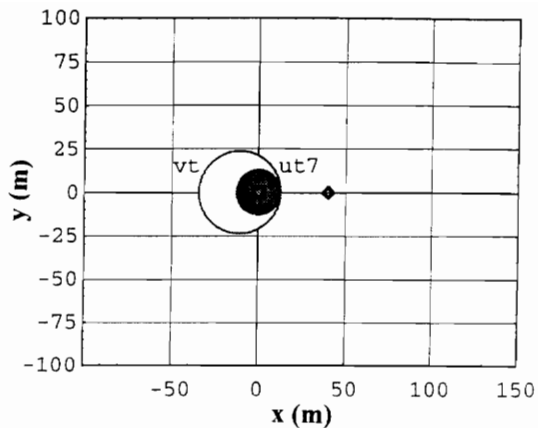


Fig. 6.3-4(b).

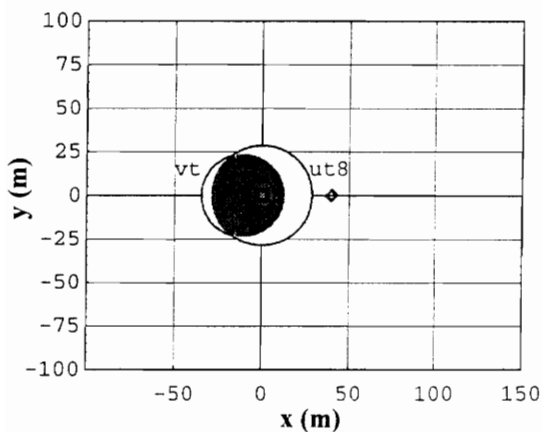


Fig. 6.3-4(c).

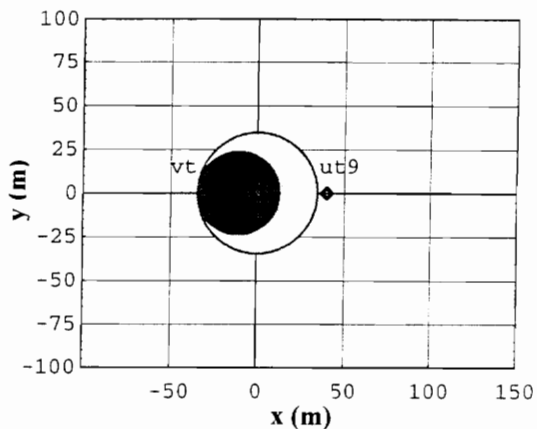


Fig. 6.3-4(d).

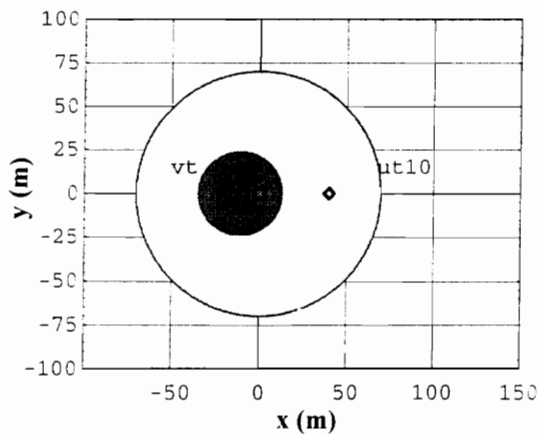


Fig. 6.3-4(e).

Fig. 6.3-4: The dark shaded areas are the coverage regions resulting from the selected values of u_i and v_i in Fig. 6.3-3. Here, S_u is *inside* the circle $U = u_i$, and S_v is also *inside* the circle $V = v_i$.

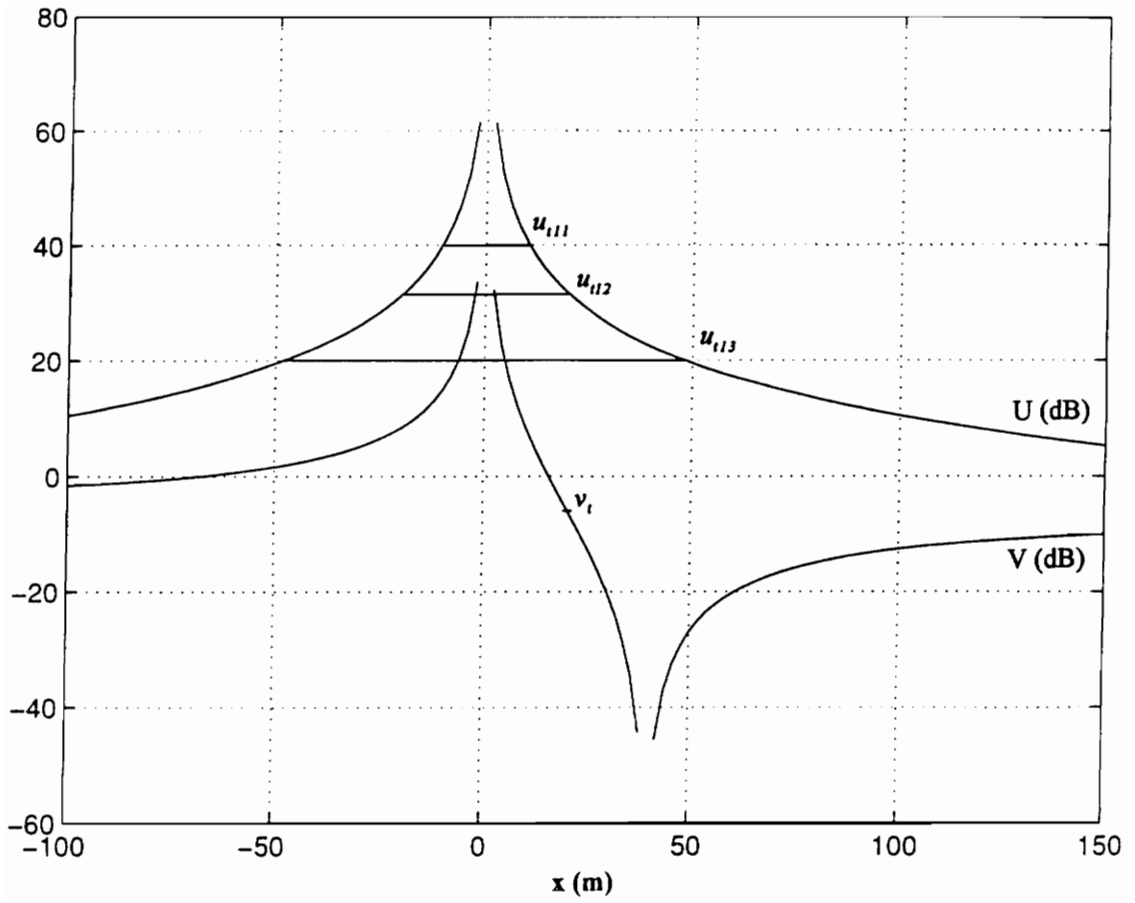


Fig. 6.3-5: Plots of U and V as a function of x . New threshold values of $U = u_{i11}, \dots, u_{i13}$ and $V = v_i$ are shown.

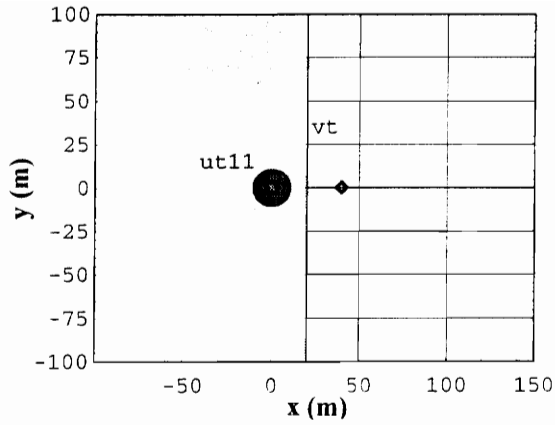


Fig. 6.3-6(a).

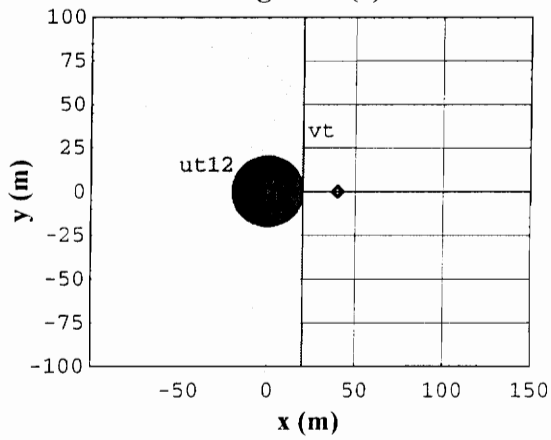


Fig. 6.3-6(b).

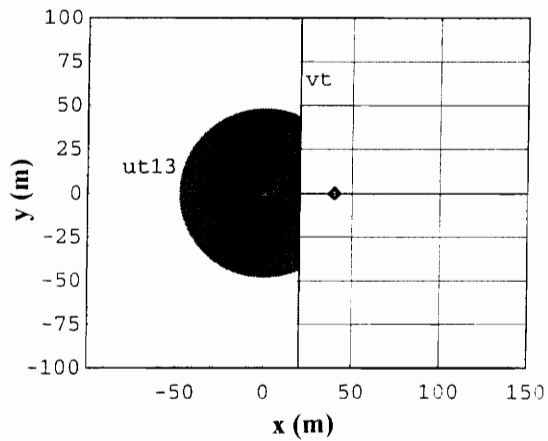


Fig. 6.3-6(c).

Fig. 6.3-6: The dark shaded areas are the coverage regions resulting from the selected values of u_i and v_i in Fig. 6.3-5. In this case also, S_u is *inside* the circle $U = u_i$, whereas S_v is the entire region to the left of $V = v_i$.

While using the SMT, it has been observed that the coverage region shown in Fig. 6.3-6(e) occurs most commonly for practical parameter values. Fig. 6.3-4(c) is also frequently obtained. For sufficiently small values of ν_i (less than 0 dB – also practically achievable), the regions shown in Figs. 6.3-2(c) and 6.3-2(e) can also result.

6.4 An Improved Search for Coverage Contours?

Using the results derived in Section 6.2, it might be possible to simplify the method of coverage region determination for use with the distance-dependent path loss model for a single interferer. The points of U and V contour intersections for the scenarios depicted in Figs. 6.3-2(b)-(d), 6.3-4(b)-(d), and 6.3-6(b)-(c) can be easily obtained by solving the following quadratic equations simultaneously:

$$x^2 + y^2 = d_i^2$$

$$\text{and } \left(x - \frac{x_i K_2^2}{K_2^2 - 1}\right)^2 + \left(y - \frac{y_i K_2^2}{K_2^2 - 1}\right)^2 = \left(\frac{x_i K_2}{K_2^2 - 1}\right)^2.$$

We now have all the information required to depict the coverage regions as discussed in Section 6.3.

Although this approach is easier, it has not been implemented in the SMT, and the elaborate procedure of solving for (3.17) at each point is followed, since this method is limited to incorporating the effect of a single interferer only. If this approach were expanded to include the effect of additional interferers, a summation of the received interferer powers at each point (according to (3.12)) and the application of (3.17) would result in almost the same communication feasibility model as the one presented in Section 3.3.

6.5 Variation in Coverage Areas

It is important to understand that Figs. 6.3-2, 6.3-4, and 6.3-6 are only approximations since these boundaries represent the *mean* values, and will, in practice, be modified by X_σ at each boundary point. However, what is important is the *behavior* of the variation of the coverage area with a change in u_t or v_t . Fig. 6.5-1 is a plot of the resulting coverage area as a function of U for several selections of v_t . The solid curves indicate the actual coverage area $S_u \cap S_v$ which differs from the theoretical coverage area S_u (shown by the dotted curve) that would have been obtained had no interferers been present. The different curves in Fig. 6.5-1 can be seen to be one of three types. Fig. 6.5-2 shows representative curves of each type.

For a given set of parameter values, we can obtain a threshold $v_t = V_T = P_t - P_i - (C/I)_{\min}$ which is the straight line in Fig. 6.2-2(b). For the values shown in Table 6.2-1, $V_T = -6$ dB.

Fig. 6.5-2(a) is a plot of coverage area versus U for $v_t = 0$ dB (greater than V_T). This curve consists of three distinct regions. Up to point A, the coverage region $S_u \cap S_v = S_u$ (corresponding to Figs. 6.3-4(a)-(b)). Beyond this point, the coverage area does continue to increase, but not as rapidly as S_u (Fig. 6.3-4(c)). This trend continues until point B is reached (Fig. 6.3-4(d)), beyond which $S_u \cap S_v = S_v$, and the area therefore remains constant, unaffected by the increase in S_u (Fig. 6.3-4(e)).

Fig. 6.5-2(b) shows the second type of curve for $v_t = V_T$. Here also, the coverage area initially increases rapidly with S_u until point A is reached (Fig. 6.3-6(b)). Beyond this point, the area still increases fairly rapidly, but this increase is not as fast as that in S_u alone (corresponding to Fig. 6.3-6(c)).

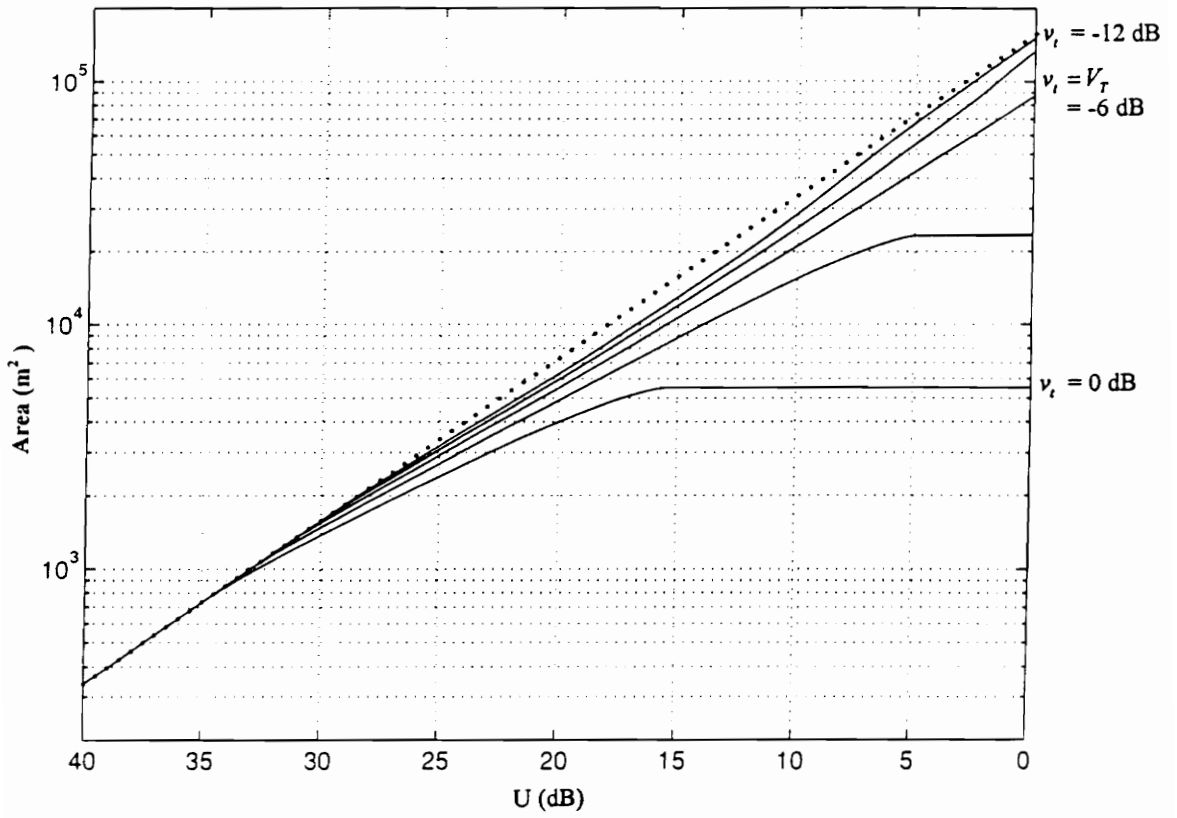


Fig. 6.5-1: Plot of coverage area ($S_u \cap S_v$) as a function of U for different v_t thresholds.

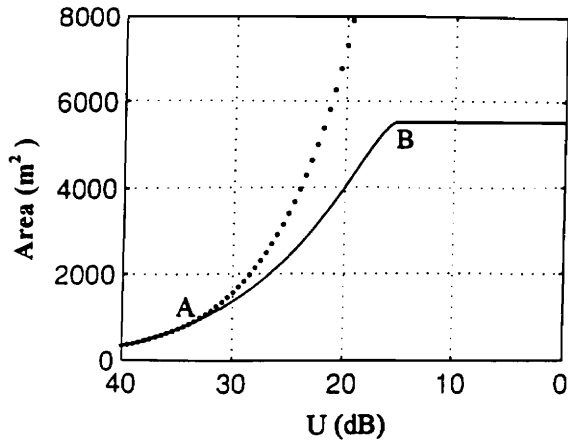


Fig. 6.5-2(a).

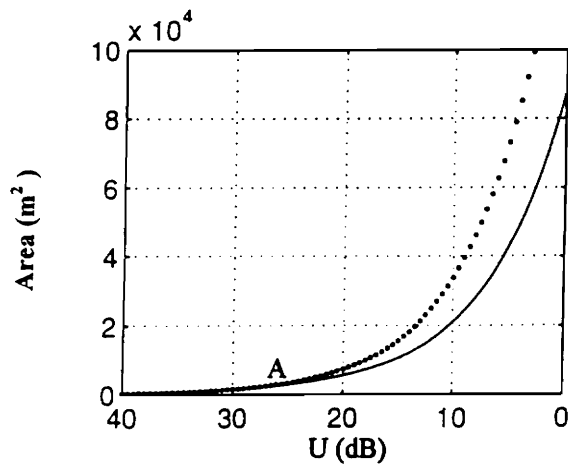


Fig. 6.5-2(b).

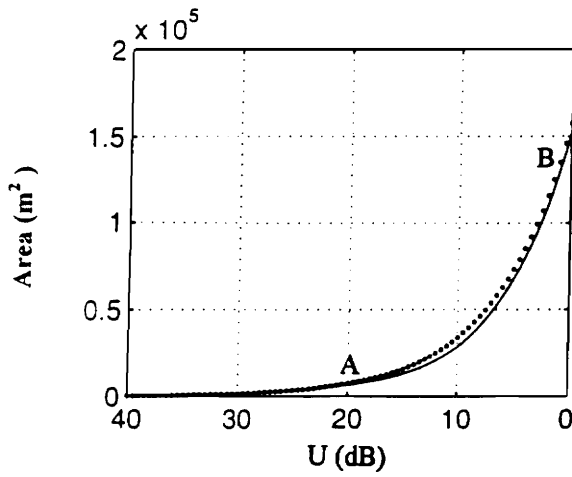


Fig. 6.5-2(c).

Fig. 6.5-2: Plot of transceiver coverage area as a function of U for (a) $v_t = 0$ dB, (b) $v_t = V_T = -6$ dB, and (c) $v_t = -12$ dB.

Finally, Fig. 6.5-2(c) shows the third type of curve in the variation of coverage area. This example curve has been obtained for $v_t = -12$ dB ($< V_T$). Initially, the coverage area increases until point A as before (Figs. 6.3-2(a)-(b)). Beyond this point, the increase in area is slowed down a little by the exclusion of $S_u \cap \bar{S}_v$ (Fig. 6.3-2(c)). This influence ends at point B (Fig. 6.3-2(d)), beyond which the area once again increases as rapidly as S_u (Fig. 6.3-2(e)).

From the above discussion, it is apparent that for practical values of V ($< v_t$), the coverage area, and therefore, system capacity is dramatically influenced by the interferer. It is now also easy to see that a change in any parameter listed in Table 6.2-1 will modify the corresponding circle/s defined by $U = u_t$ and/or $V = v_t$. As a result, any change in the coverage region or its area can be immediately visualized by referring to Figs. 6.3-2, 6.3-4, 6.3-6, and 6.5-1.

The above discussion is directly applicable to the single and multifloor distance-dependent models. In the multifloor floor attenuation factor path loss model, the quantity FAF (which is a constant for a given floor separation) can be seen as being absorbed into $PL(d_0)$, and thus affecting the plot of U by changing only its decibel level. The preceding discussion can then be applied. However, the single-floor partition attenuation factor model cannot be easily adapted to that above analysis unless we assume some symmetric uniform distribution of partitions around the transceiver.

Chapter 7.

Conclusion

This thesis report describes the Site Modeling Tool that has been developed to help predict coverage areas for wireless communication systems within buildings. The system permits the user to place transceivers and interference sources interactively within a floor plan that has been generated using AutoCAD. After placement, the user can direct the system to compute coverage regions which are highlighted directly on the floor plan. Coverage regions are calculated as a function of transceiver and interferer parameters, locations of walls and soft partitions, and building type. For versatility, all parameters are user-selectable. The system supports both single-floor and multifloor buildings.

In order to make the Site Modeling Tool interactive, relatively simple propagation models have been implemented. These models do not require computationally intensive techniques such as ray tracing. Instead, they depend only on distance and the number of intervening building partitions. The models were developed using extensive empirical measurements in earlier work, and provide useful results in many environments.

Most of the project goals listed in Section 2.1 have been satisfactorily accomplished. As required, the system is easy to use and generates impressive displays of transceiver coverage within AutoCAD floor plans. The system performs with reasonably good accuracy.

However, as is the case with the development of virtually any software tool (and even more so with an experimental tool such as the SMT), there is almost no limit to the number of enhancements or additions that can be incorporated. There are some very interesting existing and new issues that could be further addressed to enhance the utility

of the Site Modeling Tool. These could be undertaken as future work, and are outlined below.

(1) The next logical step in this research could be the automatic optimal placement of transceivers. An efficient algorithm and program that can automatically determine the number of transceivers needed and their best placement for complete coverage of a building could be developed.

(2) The system is not as fast as was initially hoped when the partition attenuation factor path loss model is used. In order to compute the coverage contour, a search is required to determine the correct location of every vertex of the contour. This search can be very time consuming if a large number of vertices are involved. During the search for a single vertex location, a large number of partitions must be examined to see which of them lie in the propagation path. Several things were attempted to increase AutoCAD's speed in doing this, but apparently most pertinent AutoCAD routines have been optimized. While other methods for improving this speed were considered, it was concluded that they were too complicated to implement during the time of the project.

Although it will probably not provide a very substantial reduction in computation speed (for reasons described in Section 5.4), the search for boundary points might be improved to be useful in the repeated iterative calculation of coverage regions of transceivers for solving the optimal location problem mentioned above.

(3) A third item that we hoped to accomplish, but which was not in our initial set of goals, is the highlighting of overlapping coverage contour regions. In its present form, the SMT displays the most recently computed coverage region over any pre-existing displayed coverage regions of other transceivers. For each transceiver, the inner coverage region is highlighted in green, and the outer coverage region is highlighted in

red, representing a guard band, hand-off, or warning area. It is easy to see that the displays can get rather confusing for more than a couple of transceivers.

For neighboring transceivers, our plan was to detect any overlapping parts of these regions and modify the color inside these areas of overlap. This seemed to be a simple problem when it was initially proposed, but turned out not to be straightforward. The problem would be fairly simple if all contours were convex. Unfortunately, nonconvex contours are quite common when the partition attenuation factor path loss model is used. Detecting the intersecting polygon(s) for two nonconvex polygons is a problem of fairly high complexity. (Notice that the intersection may take the form of several polygons.) AutoCAD does not provide a function to do this, so it would have to be implemented directly. An algorithm has been worked out, but time was not spent on writing the code because of the large number of cases that must be considered.

However, the investigation of this aspect might be inevitable if the algorithm for determining optimal transceiver location is developed, since the exact extent of overlap will have to be determined in order to quantify the overlap area.

(4) Another important enhancement that could be incorporated in the SMT is providing a choice of transmitter antenna radiation patterns. In its present form, the SMT assumes unity gain omnidirectional antennas. While this is a practical assumption for portable units, it might be desirable to include this feature for transceivers that may use directional antennas to cover specific desired regions of a floor, or prevent interference or wasteful spillover outside buildings. The software structure of the SMT would remain unchanged, but another function could be incorporated into the Environment Description module that would access a library of antenna patterns and use directional antenna gains in computing coverage regions in the Site Coverage module.

(5) The effect of interference sources on the coverage regions of a transceiver were also investigated on a theoretical basis. It was observed that the presence of interferers in the vicinity of a transceiver can dramatically alter its coverage region. The interference model (Section 3.3) can be experimentally verified using measurements.

In summary, the Site Modeling Tool is simple to use, it accommodates many different types of buildings, and it provides visual feedback that is intuitive and easy to understand. It can be used to rapidly design and help install systems, and thus satisfies an important need for system designers of indoor wireless systems.

References

- [And95] J. B. Andersen, T. S. Rappaport, and S. Yoshida, "Propagation Measurements and Models for Wireless Communications Channels," *IEEE Communications Magazine*, vol. 33, no. 1, Jan. 1995.
- [Bla93] K. L. Blackard and T. S. Rappaport, "Impulsive Noise in Personal Communication Systems," *IEEE Journal on Selected Areas in Communications*, vol. 11, no. 7, pp. 991-1000, Sep. 1993.
- [Car94] P. M. Cartwright and K. W. Sowerby, "Estimating Regions of Service in Wireless Indoor Communication Systems," *Virginia Tech 4th Symposium on Wireless Personal Communications Proceedings*, pp. 12.1-12.11, Jun. 1994.
- [Cox84] D. C. Cox, R. R. Murray, and A. W. Norris, "800 MHz Attenuation Measured in and Around Suburban Houses," *AT&T Bell Laboratories Technical Journal*, vol. 63, pp. 921-954, Jul./Aug. 1984.
- [Cox85] D. C. Cox, "Universal Portable Radio Communications," *IEEE Transactions on Vehicular Technology*, vol. 34, no. 3, pp. 117-121, Aug. 1985.
- [Dev90] D. M. J. Devasirvatham, M. J. Krain, and D. A. Rappaport, "Radio Propagation Measurements at 850 MHz, 1.7 GHz, and 4.0 GHz inside Two Dissimilar Office Buildings," *Electronics Letters*, vol. 26, no. 7, pp. 445-447, 1990.
- [Dev91] D. M. J. Devasirvatham, C. Banerjee, R. R. Murray, and D. A. Rappaport, "Four Frequency Radiowave Propagation Measurements of the Indoor Environment in a Large Metropolitan Commercial Building," *IEEE GLOBECOM '91*, Phoenix, AZ, pp. 1282-1286, Dec. 1991.
- [Has93] H. Hashemi, "The Indoor Radio Propagation Channel," *Proceedings of the IEEE*, vol. 81, no. 7, pp. 943-968, Jul. 1993.
- [Haw90] D. A. Hawbaker and T. S. Rappaport, "Indoor Wide Band Radio Wave Propagation Measurements at 1.3 GHz and 4.0 GHz," *Electronics Letters*, vol. 25, pp. 1800-1802, Oct. 1990.

- [Hon93] W. Honcharenko, H. L. Bertoni, and J. Dailing, "Mechanisms Governing Propagation Between Different Floors in Buildings," *IEEE Transactions on Antennas and Propagation*, vol. 41, no.6, pp. 787-790, Jun. 1993.
- [Laf90] J. F. Lafortune and M. Lecours, "Measurement and Modeling of Propagation Losses in a Building at 900 MHz," *IEEE Transactions on Vehicular Technology*, vol. 39, no. 2, pp. 101-108, May 1990.
- [Lee82] W. C. Y. Lee, *Mobile Communications Engineering*, McGraw-Hill, New York, 1982.
- [Mol91] D. Molkdar, "Review on Radio Propagation Into and Within Buildings," *IEEE Proceedings-H*, vol. 138, no. 1, pp. 61-73, Feb. 1991.
- [Mot88] A. J. Motley and J. M. P. Keenan, "Personal Communication Radio Coverage in Buildings at 900 MHz and 1700 MHz," *Electronics Letters*, vol. 24, no. 12, pp. 763-764, 1988.
- [Mot90] A. J. Motley and J. M. P. Keenan, "Radio Coverage in Buildings," *British Telecom Technology Journal*, Special Issue on Mobile Communications, vol. 8, no. 1, pp. 19-24, Jan. 1990.
- [Pah89] K. Pahlavan, R. Ganesh, and T. Hotaling, "Multipath Propagation Measurements on Manufacturing Floors at 910 MHz," *Electronics Letters*, vol. 25, no. 3, pp. 225-227, Feb. 1989.
- [Pan94] M. A. Panjwani, A. L. Abbott, T. S. Rappaport, and J. Haagh, "An Interactive System for Visualizing Wireless Communication Coverage within Buildings," *Virginia Tech 4th Symposium on Wireless Personal Communications Proceedings*, pp. 14.1-14.12, Jun. 1994.
- [Rap89a] T. S. Rappaport, "Indoor Radio Communications for Factories of the Future," *IEEE Communications Magazine*, pp. 15-24, May 1989.
- [Rap89b] T. S. Rappaport, "Characterization of UHF Multipath Radio Channels in Factory Buildings," *IEEE Transactions on Antennas and Propagation*, vol. 37, no. 8, pp. 1058-1069, Aug. 1989.
- [Rap91] T. S. Rappaport et al., "Statistical Channel Impulse Response Models for Factories and Open Plan Building Radio Communication System Design," *IEEE Transactions on Communications*, vol. 39, no. 5, pp. 794-806, May 1991.

- [Rap94] T. S. Rappaport and S. Sandhu, "Radio Wave Propagation for Emerging Wireless Personal Communication Systems," *Virginia Tech 4th Symposium on Wireless Personal Communications Proceedings*, pp. 1.1-1.27, Jun. 1994.
- [Sal87] A. A. M. Saleh, and R. A. Valenzuela, "A Statistical Model for Indoor Multipath Propagation," *IEEE Journal on Selected Areas in Communications*, vol. 5, no. 2, pp.128-137, Feb. 1987.
- [Sei92a] S. Y. Seidel, "Site-Specific Propagation Prediction for Wireless In-Building Personal Communications System Design," *Ph.D. dissertation*, Virginia Polytechnic Institute and State University, Blacksburg, VA, Feb. 1993.
- [Sei92b] S. Y. Seidel and T. S. Rappaport, "914 MHz Path Loss Prediction Models for Indoor Wireless Communications in Multifloored Buildings," *IEEE Transactions on Antennas and Propagation*, vol. 40, no. 2, pp. 207-217, Feb. 1992.
- [Sei92c] S. Y. Seidel, T. S. Rappaport, M. J. Feuerstein and K. L. Blackard, "The Impact of Surrounding Buildings on Propagation for Wireless In-Building Personal Communications System Design," *IEEE Vehicular Technology Conference Proceedings*, Denver, CO, pp. 814-818, May 1992.
- [Sei92d] S. Y. Seidel and T. S. Rappaport, "A Ray Tracing Technique to Predict Path Loss and Delay Spread Inside Buildings," *IEEE GLOBECOM '92*, pp. 1825-1829, Dec.1992.
- [Tuc93] B. Tuch, "Development of WaveLAN, an ISM Band Wireless LAN," *AT&T Technical Journal*, Jul./Aug. 1993.
- [Val93] R. A. Valenzuela, "A Ray Tracing Approach to Predicting Indoor Wireless Transmission," *IEEE Vehicular Technology Conference*, pp.214-218, 1993.

Appendix A: List of SMT Program Files

This appendix lists all files that comprise the SMT.

Source code:

General Files:

Smt.h

Smt.c

Environment Description Module:

Edm_bldg.h

Edm_comm.h

Channel/Communication Modules:

Comm.h

Site Coverage Module:

Scm_cntr.h

Scm_disp.h

User Interface Module:

Uim_cmd.h

Uim_dlog.h

DCL Support Files:

Afval.dcl

Alert.dcl

Chmodeq.dcl

Cntr_res.dcl

Envpar.dcl

Fafval.dcl

Faterr.dcl

Intsinfo.dcl

Nmfval.dcl

Traninfo.dcl

Transpar.dcl

Warn.dcl

Warn1.dcl

Menu Support File:

Smt.mnu

The *smt.mnu* file is simply an ASCII file that can be easily edited using any text editor. This file can be loaded by invoking the AutoCAD "menu" command. However, a more convenient alternative is to rename *smt.mnu* as *acad.mnu*. Be sure to rename and/or keep a backup of the original *acad.mnu* file before doing so. The SMT custom menus will then always be automatically loaded everytime AutoCAD is used.

Appendix B: SMT Code Compilation

The SMT was developed on a Gateway 4DX2-66V PC running AutoCAD Release 12 for Windows on Microsoft Windows (Ver. 3.1) and DOS (Ver. 6.0). Although 16 Mb of RAM was available throughout the development process, the final executable file was compiled using only 8 Mb, which is the minimum required by AutoCAD.

The Borland C++ compiler for Windows (Ver. 3.1) was used to generate the SMT executable file. The code written is upward compatible with any future releases. Due to the complexities involved in setting up the various options in the Borland C++ Interactive Development Environment (IDE), the program was compiled on a DOS command line by the *make* command. *Make.exe* accompanies the standard BC++ 3.1 distribution in the `c:\..\bcw\bin` sub-directory. The command used was

```
c:\ make -f nc.bc
```

Here, *nc.bc* is the supplied make file, which must be copied into the working directory before executing *make*. The file *nc.bc* explicitly defines options for the compiler and the linker.

Two additional files that must also be present in the working directory are *smt.rc* and *smt.def*. *Smt.rc* is the resource file for the linker. The file binds an icon and a string to the executable for display in the Windows program groups. *Smt.def* is a module definition file used to set linker options for the executable.

Library files and example make batch programs can be found in the ADS directory of AutoCAD Release 12.

AutoCAD Header Files

ADS requires the use of specially defined functions and variables, which are included in the header file *ads.h*. System definitions and controls are found in the file *adslib.h*. Also, *adscodes.h* includes declarations for constants and variables used in the program control of flow and return types. A single statement (`#include "adslib.h"`) in the beginning of the program will include all necessary files *adslib.h*, *ads.h*, *adscodes.h*, and *adsutil.h*.

File placement in the AutoCAD library path

The SMT requires that the executable and the support files (see appendix C) be placed in the AutoCAD library path, so that the full path names do not have to be specified explicitly everytime. It is recommended that the *smt.exe* file be placed in the `c:\..\acadwin\ads` sub-directory, and that the support files (*.dcl* and *.mnu*) be placed in the `c:\..\acadwin\support` sub-directory.

Vita

Manish A. Panjwani was born on October 25, 1970 in Bombay, India. He received the Bachelor of Engineering degree in Electronics (Honors) from the University of Bombay, India in July 1992. From August - December 1992, he worked with CMC Ltd. (Bombay) as an Information Technology Engineer. He received the Master of Science degree in Electrical Engineering from Virginia Polytechnic Institute and State University in May 1995. He is a member of the IEEE and the Eta Kappa Nu honor society.

Since March 1995, Mr. Panjwani has been working as a Design Engineer with LCC, L.L.C., a Washington, D.C. based wireless communications consultancy.

A handwritten signature in black ink, appearing to read 'Manish A. Panjwani', with a long horizontal stroke extending to the right.